

The geometry of Einstein-Podolsky-Rosen correlations

H. Chau Nguyen,^{1,*} Huy-Viet Nguyen,^{2,†} and Otfried Gühne^{1,‡}

¹Naturwissenschaftlich-Technische Fakultät, Universität Siegen, Walter-Flex-Straße 3, 57068 Siegen, Germany

²Institute of Physics, Vietnam Academy of Science and Technology, 10 Dao Tan, Hanoi, Vietnam

(Dated: June 27, 2019)

Correlations between distant particles are central to many puzzles and paradoxes of quantum mechanics and, at the same time, underpin various applications such as quantum cryptography and metrology. Originally in 1935, Einstein, Podolsky and Rosen (EPR) used these correlations to argue against the completeness of quantum mechanics. To formalise their argument, Schrödinger subsequently introduced the notion of quantum steering. Still, the question which quantum states can be used for EPR steering and which not remained open. Here we show that quantum steering can be viewed as an inclusion problem in convex geometry. For the case of two spin- $\frac{1}{2}$ particles, this approach completely characterises the set of states leading to EPR steering. In addition, we discuss the generalisation to higher-dimensional systems as well as generalised measurements. Our results find applications in various protocols in quantum information processing, and moreover they are linked to quantum mechanical phenomena such as uncertainty relations and the question which observables in quantum mechanics are jointly measurable.

In the simplest setting, the argument can be explained with two spin- $\frac{1}{2}$ particles, also called qubits, which are controlled by Alice and Bob at different locations [1, 2]. The particles are in the singlet state,

$$|\psi\rangle_{AB} = \frac{1}{\sqrt{2}}(|01\rangle - |10\rangle), \quad (1)$$

where $|0\rangle = |\uparrow\rangle_z$ and $|1\rangle = |\downarrow\rangle_z$ denote the two possible spin orientations in the z -direction. If Alice measures the spin of her particle in the z -direction, then, depending on the obtained result, Bob's state will be either in state $|0\rangle$ or state $|1\rangle$, due to the perfect anti-correlations of the singlet state. On the other hand, if Alice rotates her measurement device to measure the spin in the x -direction, Bob's conditional states are accordingly rotated to states $|\uparrow\rangle_x = \frac{1}{\sqrt{2}}(|0\rangle + |1\rangle)$ or $|\downarrow\rangle_x = \frac{1}{\sqrt{2}}(|0\rangle - |1\rangle)$ (see Figure 1). So, by choosing her measurement, Alice can predict with certainty both the values of z - and x -measurements on Bob's side. According to EPR, this means that both observables must correspond to "elements of reality". As the quantum mechanical formalism does not allow one to assign simultaneously definite values to these observables, EPR concluded that quantum mechanics is incomplete. As Schrödinger noted, Alice cannot transfer any information to Bob by choosing her measurement directions, but she can determine whether the wave function on his side is in an eigenstate of the Pauli matrix σ_x or σ_z . This *steering* of the wave function is, in Schrödinger's own words, "magic", as it forces Bob to believe that Alice can influence his particle from a distance [3, 4].

The situation for general quantum states other than the singlet state can be formalised as follows [5]: Alice and Bob share a bipartite quantum state ϱ_{AB} and Alice performs different measurements. For each of Alice's

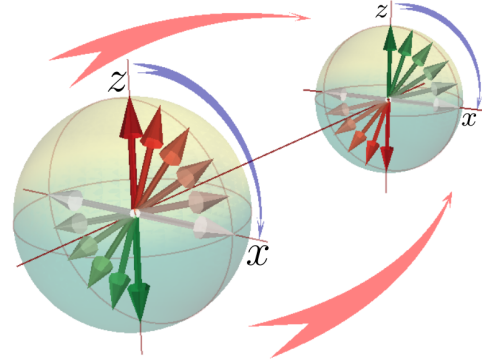


FIG. 1. Visualisation of the steering phenomenon: Alice (in the forefront) measures the spin of her particle in an arbitrary direction. Due to the quantum correlations of the singlet state, Bob's state (in the back) is projected onto the opposite direction. Bob cannot explain this phenomenon by assuming pre-existing states at his location, so he has to believe that Alice can influence his state from a distance.

measurement setting s and result r , Bob remains with a conditional state $\varrho_{r|s}$. These conditional states obey the condition $\sum_r \varrho_{r|s} = \varrho_B$, meaning that the reduced state $\varrho_B = \text{Tr}_A(\varrho_{AB})$ on Bob's side is independent of Alice's choice of measurements. However, after characterising the states $\varrho_{r|s}$, Bob may try to explain their appearance as follows: He assumes that initially his particle was in some states σ_λ with probability $p(\lambda)$, parametrised by some parameter λ . Then, Alice's measurement and result just gave him additional information on the probability of the states. This leads to states of the form [5]

$$\varrho_{r|s} = p(r|s) \int d\lambda p(\lambda|r, s) \sigma_\lambda. \quad (2)$$

This can be interpreted as if the probability distribution $p(\lambda)$ is just updated to $p(\lambda|r, s)$, depending on the classical information about the result and setting r, s . If a

* chau.nguyen@uni-siegen.de

† nhviet@iop.vast.ac.vn

‡ otfried.guehne@uni-siegen.de

representation as in equation (2) exists, Bob does not need to assume any kind of action at a distance to explain the post-measurement states $\varrho_{r|s}$. Consequently, he does not need to believe that Alice can steer his state by her measurements and one also says that the state ϱ_{AB} is *unsteerable* or has a local hidden state (LHS) model. If such a model does not exist, Bob is required to believe that Alice can steer the state in his laboratory by some action at a distance. In this case, the state is said to be *steerable*.

So far, EPR steering has been observed in several experiments [6–13], but the question which states can be used for EPR steering and which not remained, despite considerable theoretical effort [14–28], open. It is known that the set of steerable quantum states is strictly smaller than the set of entangled states and strictly larger than the set of states leading to a Bell inequality violation. But both entanglement and Bell nonlocality are not well understood [29, 30]; only for the case of small dimensions or special families of states the famous Peres-Horodecki criterion provides an exact characterisation of the entangled states [31, 32]. In this paper we present a solution to the problem of steerability for the case of projective measurements carried out on two qubits. The generalisation of the technique to higher-dimensional systems as well as taking into account generalised measurements is possible.

Conditional states and LHS models.— Let us characterise the conditional states and possible LHS models. For the former, we note that any bipartite quantum state ϱ_{AB} defines a map Λ from operators on Alice’s space to operators on Bob’s space via

$$\Lambda(X_A) = \text{Tr}_A(\varrho_{AB} X_A \otimes \mathbb{1}_B). \quad (3)$$

This map characterises the conditional states as follows: A result of a measurement setting is described by an effect $E_{r|s}$ which is an operator with positive eigenvalues not larger than one. The conditional state is then just given by $\varrho_{r|s} = \text{Tr}_A(\varrho_{AB} E_{r|s} \otimes \mathbb{1}_B) = \Lambda(E_{r|s})$.

For our approach it is important that Λ has a clear geometrical meaning (see Figure 2). The set of measurement effects on Alice’s side, denoted by $\mathcal{M}_A = \{E_{r|s} \mid 0 \leq E_{r|s} \leq \mathbb{1}_A\}$, is a four-dimensional double cone, where 0 and $\mathbb{1}_A$ correspond to the south- and north pole, and the pure effects of the form $E_{r|s} = |\psi\rangle\langle\psi|$ constitute the equator, which is nothing but Alice’s Bloch sphere. The map Λ is linear and maps this double cone to a smaller double cone, denoted by $\Lambda(\mathcal{M}_A)$, which we call the *set of steering outcomes* [20]. For our purposes, we can assume without loss of generality that the map Λ is invertible; the proof of this and all forthcoming mathematical statements, can be found in the Appendix [33].

Let us now characterise the set of all possible LHS models. We first restrict our attention to projective measurements on two qubits, later we discuss the general case. Projective measurements are described by two orthogonal projectors $E_{+|s}$ and $E_{-|s}$ summing up to the identity, $E_{+|s} + E_{-|s} = \mathbb{1}_A$. It is known that the LHS

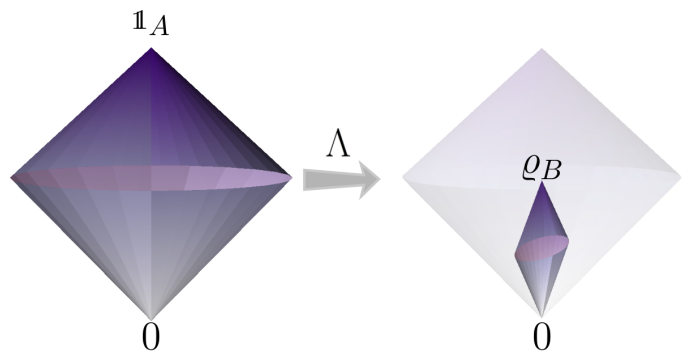


FIG. 2. Geometrical view of the map Λ : The set of measurement effects \mathcal{M}_A on Alice’s side is a four-dimensional double cone, where 0 and $\mathbb{1}_A$ correspond to the south- and north pole and the equator is formed by the Bloch sphere. Under the action of the linear map Λ this double cone is mapped onto a subset of itself, with $\Lambda(0) = 0$ and $\Lambda(\mathbb{1}_A) = \varrho_B$. The resulting set of steering outcomes is completely characterised by ϱ_B and the image of the equator under Λ .

model (2) can be rewritten as [27]

$$\varrho_{\pm|s} = \Lambda(E_{\pm|s}) = \int_{\sigma \in \mathcal{B}_B} d\mu(\sigma) G_{\pm|s}(\sigma) \sigma, \quad (4)$$

with an integration over a probability distribution μ over all pure and mixed states in Bob’s Bloch ball \mathcal{B}_B . The so-called response functions $G_{\pm|s}(\sigma)$ are positive and normalised as $G_{+|s} + G_{-|s} = 1$, which implies that they always have to obey the minimal requirement

$$\varrho_B = \Lambda(\mathbb{1}_A) = \int_{\sigma \in \mathcal{B}_B} d\mu(\sigma) \sigma. \quad (5)$$

In this scenario the set of all conditional states $\varrho_{\pm|s}$ that can be modelled with an LHS model is characterised by the probability distribution μ only. We call this set the *capacity* of μ and denote it by [20, 27]

$$\mathcal{K}(\mu) = \left\{ K = \int_{\sigma \in \mathcal{B}_B} d\mu(\sigma) g(\sigma) \sigma : 0 \leq g(\sigma) \leq 1 \right\}. \quad (6)$$

The geometric approach.— In order to decide steerability, one has to compare the set of steering outcomes with the possible capacities. If one finds an LHS ensemble μ for which $\Lambda(\mathcal{M}_A)$ is a subset of $\mathcal{K}(\mu)$, then ϱ_{AB} is not steerable. On the other hand, if $\mathcal{K}(\mu)$ does not cover $\Lambda(\mathcal{M}_A)$ for all μ , then ϱ_{AB} is steerable.

Checking the inclusion relation between these sets is simplified by geometry, see Figure 3. $\mathcal{K}(\mu)$ is a convex set which contains 0 and ϱ_B . The double cone $\Lambda(\mathcal{M}_A)$ is contained in this set if and only if its equator is contained in $\mathcal{K}(\mu)$. If we choose the metric appropriately, the equator of $\Lambda(\mathcal{M}_A)$ is a ball of radius one. Whether $\mathcal{K}(\mu)$ contains the ball or not, can thus be determined by calculating the *principal radius*, defined as the minimal distance from the boundary of $\mathcal{K}(\mu)$ in the equator hyperplane to the centre of the ball [22].

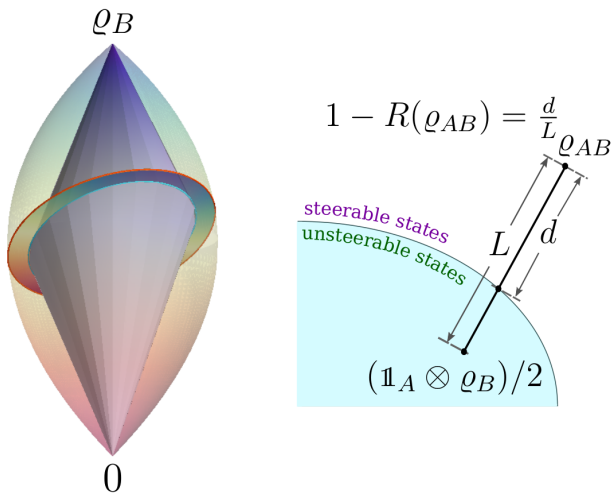


FIG. 3. (left) The geometrical interpretation of the critical radius: The capacity $\mathcal{K}(\mu)$ is a convex set containing 0 and ϱ_B . The double cone $\Lambda(\mathcal{M}_A)$ has 0 and ϱ_B as south- and north pole, so $\Lambda(\mathcal{M}_A)$ is contained in $\mathcal{K}(\mu)$ if and only if its equator (cyan) is in $\mathcal{K}(\mu)$. This can be checked by computing the radius of $\mathcal{K}(\mu)$ in the appropriate plane and metric (red). (right) Operational meaning of the critical radius: $1 - R(\varrho_{AB})$ measures the distance from ϱ to the surface of unsteerable/steerable states relatively to $(\mathbb{1}_A \otimes \varrho_B)/2$.

Our first main result is that the principal radius for a given probability distribution can be computed as a simple optimisation problem, given by

$$r(\varrho_{AB}, \mu) = \min_C \frac{1}{\sqrt{2} \|\text{Tr}_B[\bar{\varrho}(\mathbb{1}_A \otimes C)]\|} \int_{\sigma \in \mathcal{B}_B} d\mu(\sigma) |\text{Tr}_B(C\sigma)|, \quad (7)$$

where $\bar{\varrho} = \varrho_{AB} - (\mathbb{1}_A \otimes \varrho_B)/2$, the norm is given by $\|X\| = \sqrt{\text{Tr}(X^\dagger X)}$, and the minimisation runs over all single-qubit observables C on Bob's space. The proof of Eq. (7) relies on the Bloch representation and is given in the Appendix [33].

Equation (7) allows us to compute the principal radius for a given distribution μ over states in Bob's Bloch ball. It remains to maximise this over all possible probability distributions. This leads to the *critical radius*

$$R(\varrho_{AB}) = \max_{\mu} r(\varrho_{AB}, \mu). \quad (8)$$

In this way, we have reduced the characterisation of steering to the computation of the critical radius and we can formulate: *A two-qubit state can be used for EPR steering, if and only if the critical radius is smaller than one.* All that remains to be done is to characterise the critical radius and to provide efficient methods for computing it. Showing the existence of the maximum in Eq. (8) requires careful continuity arguments as explained in the Appendix [33].

Properties of the critical radius. — The first interesting property of the critical radius is its *scaling*. Given a two-qubit state, we can consider a family of states by mixing

it with a special kind of separable noise,

$$\varrho_{\alpha}^{\text{noise}} = \alpha \varrho_{AB} + (1 - \alpha) \frac{\mathbb{1}_A}{2} \otimes \varrho_B, \quad (9)$$

where $0 \leq \alpha \leq 1$. For these states, we can show that

$$R(\varrho_{\alpha}^{\text{noise}}) = \frac{1}{\alpha} R(\varrho_{AB}). \quad (10)$$

This implies that computing the critical radius for ϱ_{AB} also gives its values on the entire line in the state space parametrised by $\varrho_{\alpha}^{\text{noise}}$. This scaling sheds light on the operational meaning of the critical radius: $1 - R(\varrho_{AB})$ measures the distance from ϱ_{AB} along this line to the border between steerable and unsteerable states relatively to $(\mathbb{1}_A \otimes \varrho_B)/2$.

The second important property is the *symmetry* of the critical radius. Given a state ϱ_{AB} , we consider the family of states

$$\tilde{\varrho}_{AB} = \frac{1}{\mathcal{N}} (U_A \otimes V_B) \varrho_{AB} (U_A^\dagger \otimes V_B^\dagger), \quad (11)$$

where U_A is a unitary matrix on Alice's side, V_B is an invertible matrix on Bob's side, and \mathcal{N} denotes the normalisation. For this family of states one can show that $R(\varrho_{AB}) = R(\tilde{\varrho}_{AB})$. This symmetry of the critical radius thus generalises and formalises quantitatively the early observation that the existence of an LHS model is invariant under Alice's local unitary and Bob's local filtering operations [18, 19, 48]. One may ask to which extent a mixed two-qubit state can be simplified with transformations as in equation (11). The answer is that any entangled state can be brought into a canonical form without changing its critical radius. In the canonical form, $\varrho_B = \mathbb{1}_B/2$ is maximally mixed and, in addition, all two-body correlations vanish, up to the diagonal ones, $s_i = \text{Tr}(\varrho_{AB} \sigma_i \otimes \sigma_i)$ for $i = x, y, z$. So the critical radius of a state is uniquely determined by six parameters, coming from the reduced state of Alice, parametrised by $a_i = \text{Tr}(\varrho_{AB} \sigma_i \otimes \mathbb{1}_B)$ and by a diagonal 3×3 -matrix T .

Some facts about steering follow directly from the two properties mentioned above. First, as any pure entangled state $|\psi\rangle$ is equivalent to a Bell state in the sense of equation (11), one can easily show that $R(|\psi\rangle\langle\psi|) = 1/2$. Second, the previous properties allow for characterising the convex sets $Q_t = \{\varrho_{AB} : R(\varrho_{AB}) \geq t\}$ and one can, for some cases, compute the tangent hyperplanes, resulting in optimal steering inequalities. Finally, generalising equation (11), R is also invariant under the inversion of the Bloch sphere of either of the parties. This is rather surprising as entanglement of two-qubit states is equivalent to the occurrence of negative eigenvalues after partial transposition [31, 32], which can be seen as a local inversion of the Bloch sphere. So, entanglement and quantum steering are, in fact, types of quantum correlations with fundamentally different mathematical structures.

Computation of the critical radius. — For practical convenience, the calculation of the critical radius of a generic state is carried out starting from its canonical form.

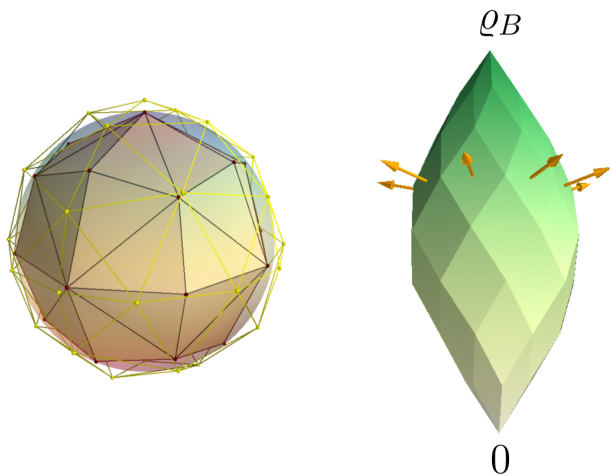


FIG. 4. (left) In order to characterise all probability distributions on the Bloch sphere, one can use inner and outer approximations of the sphere by polytopes. For the polytopes and the optimisation problem in equation (7) it suffices to consider probability distributions supported at the extremal points. (right) For a given polytope, the capacity $\mathcal{K}(\mu)$ is a polytope again. Consequently, when computing the principal radius it suffices to consider the (finite) set of directions corresponding to the faces of the capacity polytope.

Then, in order to evaluate equation (8) one needs to characterise the possible distributions μ . Instead of maximising over all probability distributions on the Bloch ball, we approximate the ball by inner or outer polytopes as illustrated in Figure 4. Crucially, for the special function in equation (7) one can show that optimising over probability distributions supported at the vertices of the outer (inner) polytope leads to an upper (lower) bound R_{out} (R_{in}) for the critical radius. One may even simplify the calculation: If the inner polytope is chosen to have inversion symmetry, one has $R_{\text{in}} \leq R(\varrho_{AB}) \leq R_{\text{in}}/r_{\text{in}}$, where r_{in} is the inscribed radius of the polytope. Then the relative difference between the bounds depends on the polytope only and not on details of the state. This bound also shows that as r_{in} converges to 1 one obtains an asymptotically exact value for $R(\varrho_{AB})$.

For a given polytope with N vertices, the calculation of the critical radius proceeds as follows: The capacity $\mathcal{K}(\mu)$ is a polytope in the four-dimensional space with $O(N^3)$ facets. When computing the critical radius, it suffices to consider the finite set of operators C that correspond to normal vectors of these facets, and these operators do not depend on the probability distribution on the polytope. As a consequence, the optimisation over probability distributions is formulated as a linear program of finite size.

To illustrate the power of the method, we show examples of two-dimensional random cross-sections of the set of two-qubit states, see Figure 5. We observe that the computed upper and lower bounds for the critical radius are very tight even when a polytope with 252 vertices was used. A detailed discussion including further examples of

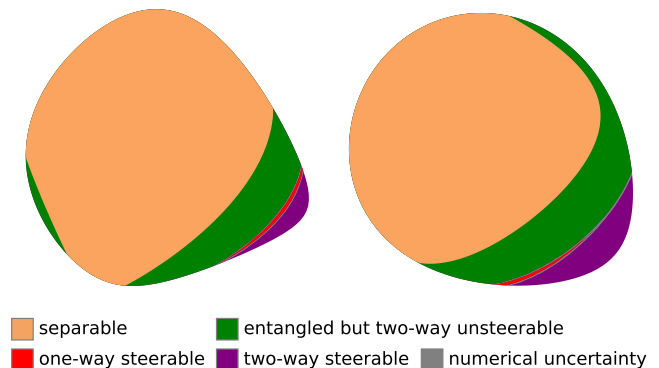


FIG. 5. Two two-dimensional random cross-sections of the set of all two-qubit states. As EPR steering is not symmetric under the exchange of Alice and Bob, one can distinguish different classes of steerable states. The colours denote the set of separable states (characterised by the partial transposition [31, 32]), entangled states that are unsteerable, one-way steerable states (Alice to Bob or vice versa), and two-way steerable states (Alice to Bob and vice versa). The very thin grey areas denote the states where the used numerical precision was not sufficient to make an unambiguous decision.

states is given in the Appendix [33].

Prior to our work, certain necessary and sufficient conditions for steering were proposed [25, 26], however their computability cannot be generally illustrated. There have been also attempts in estimating the boundary of the set of unsteerable states for special families of states with semidefinite programming (SDP) [16, 23, 28, 47]. However, the SDP size increases exponentially with the number of measurements used to approximate the set of all measurements. This limitation hinders the accurate locating of the boundary even for special choices of cross-sections. Contrary to that, here we obtained a linear program, of which the size increases cubically with the number of approximated points. Both lower bound and upper bound with a pre-defined difference less than 1% for the critical radius of a generic state can be easily obtained in a reasonable computational time. Our implementation is available at a public repository [46].

Finally, we note that certain analytical bounds for the critical radius can also be derived from our approach. For example, for a state in the canonical form, it can be shown that

$$2\pi N_T |\det(T)| \geq R(\varrho_{AB}) \geq \frac{2\pi N_T |\det(T)|}{1 + \|T^{-1}\vec{a}\|}, \quad (12)$$

where $\vec{a} = (a_x, a_y, a_z)$ is the Bloch vector of Alice's reduced state, $N_T^{-1} = \int dS(\vec{n}) [\vec{n}^T T^{-2} \vec{n}]^{-2}$ and the integration runs over the surface of the unit sphere. If $\vec{a} = 0$, these bounds recover the exact formula for the critical radius of Bell diagonal states [21, 22].

Generalised measurements and higher-dimensional systems. — A similar formula for the principal and critical radius can be derived for generalised measurements

(i. e., positive operator-valued measures—POVMs) and higher-dimensional systems, despite their more complicated geometry. As we explain in the Appendix [33], many properties of the critical radius, such as its scaling and its symmetry still hold. The fundamental question arises whether generalised measurements are more useful for steering than the standard projective measurements considered so far. For two qubits, numerical estimation of the principal radii for POVMs provides clear evidence that, for a generic probability distribution μ , the principal radius for POVMs is the same as that for projective measurements. This encourages us to conjecture that POVMs do not give any advantage in EPR steering for the case of two-qubit states.

Discussion.— EPR steering is an asymmetric phenomenon where Bob, contrary to Alice, has well characterised measurements. Consequently the underlying correlations find applications in non-symmetric scenarios of quantum information processing, such as one-sided device-independent quantum key distribution [49] or sub-channel discrimination [50]. Clearly, our solution to the steering problem helps to understand and optimise these applications and their experimental realisations.

In addition, there are far-ranging consequences. First, it has been established that steering is in one-to-one correspondence with the question which measurements in

quantum mechanics can be jointly measured [48, 51–53]. Second, recent works established close connections between quantum steering and entropic uncertainty relations [54, 55]. Joint measurability and entropic uncertainty relations are central for many applications of quantum physics, such as the security of quantum key distribution [56]. We expect that our results and methods presented here may shed new light on these topics in the near future.

Acknowledgements.— We are grateful to Fabian Bernards, Francesco Buscemi, Shuming Cheng, Ana C. S. Costa, Michael J. W. Hall, Teiko Heinosaari, C. Jebaratnam, Sania Jevtic, X. Thanh Le, Antony Milne, V. Anh Nguyen, Q. Dieu Nguyen, Jiangwei Shang, Roope Uola, Howard M. Wiseman, Xiao-Dong Yu, and particularly N. Duc Le for helpful comments and discussions. We thank the authors of Ref. [28] for kindly providing us with their SDP data. This work was supported by the DFG and the ERC (Consolidator Grant 683107/TempoQ). CN also acknowledges the support by the Vietnam National Foundation for Science and Technology Development (NAFOSTED) under grant number 103.02-2015.48. HVN acknowledges the financial support of the International Centre of Physics at the Institute of Physics, Vietnam Academy of Science and Technology.

-
- [1] A. Einstein, B. Podolsky, and N. Rosen, *Phys. Rev.* **47**, 777 (1935).
- [2] D. Bohm, *Quantum Theory* (Prentice Hall, New York, 1951).
- [3] E. Schrödinger, letter to A. Einstein on 13th July 1935, reprinted in K. v. Meyenn (ed.), *Eine Entdeckung von ganz außerordentlicher Tragweite*, Springer (2011).
- [4] E. Schrödinger, *Proc. Camb. Phil. Soc.* **31**, 555 (1935).
- [5] H. M. Wiseman, S. J. Jones, and A. C. Doherty, *Phys. Rev. Lett.* **98**, 140402 (2007).
- [6] B. Wittmann, S. Ramelow, F. Steinlechner, N. K. Langford, N. Brunner, H. Wiseman, R. Ursin, and A. Zeilinger, *New J. Phys.* **14**, 053030 (2012).
- [7] D. J. Saunders, S. J. Jones, H. M. Wiseman, and G. J. Pryde, *Nature Phys.* **6**, 845 (2010).
- [8] V. Händchen, T. Eberle, S. Steinlechner, A. Sambrowski, T. Franz, R. F. Werner, and R. Schnabel, *Nature Phot.* **6**, 596 (2012).
- [9] D.H. Smith, G. Gillett, M. de Almeida, C. Branciard, A. Fedrizzi, T. J. Weinhold, A. Lita, B. Calkins, T. Gerrits, H. M. Wiseman, S. W. Nam, and A. G. White, *Nature Comm.* **3**, 625 (2012).
- [10] A. J. Bennet, D. A. Evans, D. J. Saunders, C. Branciard, E. G. Cavalcanti, H. M. Wiseman, and G. J. Pryde, *Phys. Rev. X* **2**, 031003 (2012).
- [11] N. Tischler, F. Ghafari, T. J. Baker, S. Slussarenko, R. B. Patel, M. M. Weston, S. Wollmann, L. K. Shalm, V. B. Verma, S. W. Nam, H. C. Nguyen, H. M. Wiseman, and G. J. Pryde, *Phys. Rev. Lett.* **121**, 100401 (2018).
- [12] K. Sun, X.-J. Ye, J.-S. Xu, X.-Y. Xu, J.-S. Tang, Y.-C. Wu, J.-L. Chen, C.-F. Li, and G.-C. Guo *Phys. Rev. Lett.* **116**, 160404 (2016).
- [13] Y. Xiao, X.-J. Ye, K. Sun, J.-S. Xu, C.-F. Li, and G.-C. Guo *Phys. Rev. Lett.* **118**, 140404 (2017).
- [14] S. J. Jones, H. M. Wiseman, A. C. Doherty, *Phys. Rev. A* **76**, 052116 (2007).
- [15] M. F. Pusey, *Phys. Rev. A* **88**, 032313 (2013).
- [16] P. Skrzypczyk, M. Navascues, and D. Cavalcanti, *Phys. Rev. Lett.* **112**, 180404 (2014).
- [17] J. Bowles, T. Vertesi, M. Tulio Quintino, and N. Brunner, *Phys. Rev. Lett.* **112**, 200402 (2014).
- [18] R. Gallego and L. Aolita, *Phys. Rev. X* **5**, 041008 (2015).
- [19] M. Tulio Quintino, T. Vértesi, D. Cavalcanti, R. Augusiak, M. Demianowicz, A. Acín, and N. Brunner, *Phys. Rev. A* **92**, 032107 (2015).
- [20] H. C. Nguyen and T. Vu, *Phys. Rev. A* **94**, 012114 (2016).
- [21] S. Jevtic, M. J. W. Hall, M. R. Anderson, M. Zwiernik and H. M. Wiseman *J. Opt. Soc. Am. B* **32**, A40 (2015).
- [22] H. C. Nguyen and T. Vu, *Europhys. Lett.* **155**, 10003 (2016).
- [23] D. Cavalcanti and P. Skrzypczyk, *Rep. Prog. Phys.* **80**, 024001 (2017).
- [24] A. Rutkowski, A. Buraczewski, P. Horodecki, and M. Stobiska, *Phys. Rev. Lett.* **118**, 020402 (2017).
- [25] B.-C. Yu, Z.-A. Jia, Y.-C. Wu, and G.-C. Guo, *Phys. Rev. A* **97**, 012130 (2018).
- [26] B.-C. Yu, Z.-A. Jia, Y.-C. Wu, and G.-C. Guo, *Phys. Rev. A* **98**, 052345 (2018).
- [27] H.C. Nguyen, A. Milne, T. Vu, and S. Jevtic, *J. Phys. A: Math. Theor.* **51**, 355302 (2018).
- [28] M. Filleltaaz, F. Hirsch, S. Designolle, and N. Brunner, *Phys. Rev. A* **98**, 022115 (2018).

- [29] R. Horodecki, P. Horodecki, M. Horodecki, and K. Horodecki, *Rev. Mod. Phys.* **81**, 865 (2009).
- [30] N. Brunner, D. Cavalcanti, S. Pironio, V. Scarani, and S. Wehner, *Rev. Mod. Phys.* **86**, 419 (2014).
- [31] A. Peres, *Phys. Rev. Lett.* **77**, 1413 (1996).
- [32] M. Horodecki, P. Horodecki, and R. Horodecki, *Phys. Lett. A* **223**, 1 (1996).
- [33] The Appendices can be found in the Supplementary Material, which include references [34-45]
- [34] Private communication with Sania Jevtic.
- [35] E. Schrödinger, *Proc. Cambridge Philos. Soc.* **32**, 446 (1936).
- [36] N. Gisin, *Helvetica Physica Acta* **62**, 363 (1989).
- [37] L. P. Hughston, R. Jozsa, and W. K. Wootters, *Phys. Lett. A* **183**, 14 (1993).
- [38] V. Bogachev, *Measure Theory I & II*, Springer-Verlag, Berlin (2007).
- [39] R. T. Rockafellar, *Convex analysis*, Princeton University Press (1970).
- [40] S. Jevtic, M. F. Pusey, D. Jennings, and T. Rudolph, *Quantum Steering Ellipsoids* *Phys. Rev. Lett.* **113**, 020402 (2014).
- [41] J. Bowles, F. Hirsch, M. T. Quintino and N. Brunner, *Phys. Rev. A* **93**, 022121 (2016).
- [42] K. R. Parthasarathy, *Probability Measures on Metric Spaces*, Academic Press Inc., New York & London (1967).
- [43] R. F. Werner, *J. Phys. A: Math. Theor.*, **47**, 424008 (2014).
- [44] J. Barrett, *Phys. Rev. A* **65**, 042302 (2002).
- [45] R. H. Hardin, N. J. A. Sloane and W. D. Smith, Tables of spherical codes with icosahedral symmetry, published electronically at <http://NeilSloane.com/icosahedral.codes/>.
- [46] Gitlab repository: <https://gitlab.com/cn611340/epr-steering>
- [47] D. Cavalcanti, L. Guerini, R. Rabelo, and P. Skrzypczyk, *Phys. Rev. Lett.* **117**, 190401 (2016).
- [48] R. Uola, T. Moroder, and O. Gühne, *Phys. Rev. Lett.* **113**, 160403 (2014).
- [49] C. Branciard, E. G. Cavalcanti, S. P. Walborn, V. Scarani, and H. M. Wiseman, *Phys. Rev. A* **85**, 010301(R) (2012).
- [50] M. Piani and J. Watrous, *Phys. Rev. Lett.* **114**, 060404 (2015).
- [51] M. T. Quintino, T. Vertesi, and N. Brunner, *Phys. Rev. Lett.* **113**, 160402 (2014).
- [52] R. Uola, C. Budroni, O. Gühne, and J.-P. Pellonpää, *Phys. Rev. Lett.* **115**, 230402 (2015).
- [53] T. Heinosaari, J. Kiukas, D. Reitzner, and J. Schultz, *J. Phys. A: Math. Theor.* **48**, 435301 (2015).
- [54] A.C.S. Costa, R. Uola, and O. Gühne, *Phys. Rev. A* **98**, 050104 (2018).
- [55] T. Krivachy, F. Fröwis, and N. Brunner, *Phys. Rev. A* **98**, 062111 (2018).
- [56] P.J. Coles, M. Berta, M. Tomamichel, and S. Wehner, *Rev. Mod. Phys.* **89**, 015002 (2017).

Supplementary Material

CONTENTS

A. The geometry of the state space	7
B. Measurement outcomes and steering outcomes	8
C. The capacity of an LHS ensemble	8
D. The minimal requirement and the principal radius	8
E. A simple formula for the critical radius of two qubits	8
F. Relaxing the non-degeneracy condition of the state	10
G. Defining domain of the principal radius	10
H. Concavity of the principal radius	10
I. Upper-semicontinuity of the principal radius	10
J. Existence of an optimal LHS ensemble	11
K. Implication of symmetry on the optimal LHS ensemble	11
L. Scaling of the critical radius	11
M. Continuous symmetry of the critical radius	12
N. Time-reversal symmetry of the critical radius	12
O. The canonical form and normal states	13
P. Lower-semicontinuity of the principal radius	14
Q. Finiteness of the critical radius	15
R. Continuity of the critical radius	15
S. Levels of the critical radius	16
T. Analytic formula of the critical radius for certain states	17
1. Product states	17
2. T-states	18
3. Some analytical bounds for the critical radius	18
U. Computation of the critical radius	19
1. Bringing the state to the canonical form	19
2. Sandwiching the Bloch sphere between two polytopes	19
3. Universal bound of the relative error	21
4. Optimise the principal radius over probability distributions on a polytope	22

5. Implication of the symmetry of the state	22
6. Remark on the computation for degenerate states	22
7. Technical aspects and the EPR-package	23
V. Gradients of the critical radius	23
W. Details of the examples	24
1. Random cross-sections	24
2. Symmetric cross-sections	24
3. A family of one-way unsteerable states	25
X. Generalisation to higher dimensional systems	26
1. Reducing to the formula for two-qubit states	26
2. Remarks on other properties	26
a. Scaling of the critical radius	27
b. Continuous symmetry of the critical radius	27
Y. On the relation between PVMs and POVMs	27

Appendix A: The geometry of the state space

To fix the notation, we consider a state of two qubits AB , that is, a positive (semi-definite) unit-trace operator ϱ over $\mathcal{H}_A \otimes \mathcal{H}_B$, where \mathcal{H}_A and \mathcal{H}_B are 2-dimensional (2D) Hilbert spaces. The spaces of hermitian operators acting on \mathcal{H}_A and \mathcal{H}_B are denoted by $B^H(\mathcal{H}_A)$ and $B^H(\mathcal{H}_B)$, respectively, with the identity operators $\mathbb{1}_A$ and $\mathbb{1}_B$.

Note that $B^H(\mathcal{H}_A)$ is a 4-dimensional (4D) Euclidean space with the Hilbert-Schmidt inner product, $\langle X, Y \rangle = \text{Tr}(XY)$ for $X, Y \in B^H(\mathcal{H}_A)$. If one chooses an orthonormal basis for \mathcal{H}_A , and uses the Pauli matrices $\{\sigma_i^A\}_{i=0}^3$ (with $\sigma_0^A = \mathbb{1}_A$) as the basis of $B^H(\mathcal{H}_A)$, any operator X of $B^H(\mathcal{H}_A)$ can be written as

$$X = \frac{1}{2} \sum_{i=0}^3 x_i \sigma_i^A, \quad (\text{A1})$$

where $x_i = \text{Tr}(X\sigma_i^A)$. We will refer to this basis as the Pauli basis.

One can also use the Pauli basis for $B^H(\mathcal{H}_B)$. With these two coordinate systems, a density operator ϱ can then be written in terms of the Bloch tensor,

$$\varrho = \frac{1}{4} \sum_{i,j=0}^3 \Theta_{ij} \sigma_i^A \otimes \sigma_j^B, \quad (\text{A2})$$

where $\Theta_{ij} = \text{Tr}[\varrho(\sigma_i^A \otimes \sigma_j^B)]$. The Bloch tensor is usually written as a matrix

$$\Theta = \begin{pmatrix} 1 & \mathbf{b}^T \\ \mathbf{a} & T \end{pmatrix}, \quad (\text{A3})$$

where \mathbf{a} and \mathbf{b} are Alice's and Bob's Bloch vectors, and T is their correlation matrix.

The map Λ from Alice's side, $\Lambda : B^H(\mathcal{H}_A) \rightarrow B^H(\mathcal{H}_B)$, is defined by

$$\Lambda(X) = \text{Tr}_A[\varrho(X \otimes \mathbb{1}_B)] \quad (\text{A4})$$

for $X \in B^H(\mathcal{H}_A)$. The Bloch tensor also allows for a direct representation of Alice's map Λ as a (4×4) matrix,

$$\Lambda \equiv \frac{1}{2}\Theta^T. \quad (\text{A5})$$

We say a state ϱ is *degenerate* if the map Λ is degenerate, i. e., non invertible. Otherwise it is said to be *non-degenerate*. We note that degenerate states are zero-measured in the set of all states. Moreover, they are separable [34] (see Section U 6). As separable states cannot be used for steering, we can, without loss of generality, always assume states to be non-degenerate. We do often make side remarks on how to cope with degenerate states for completeness.

Appendix B: Measurement outcomes and steering outcomes

The set of Alice's *measurement outcomes* is defined by $\mathcal{M}_A = \{X \in B^H(\mathcal{H}_A) : 0 \leq X \leq \mathbb{1}_A\}$. Under the map Λ , Alice's measurement outcome set is mapped to the set of Alice's *steering outcomes*, $\Lambda(\mathcal{M}_A) \subseteq B^H(\mathcal{H}_B)$. Note that our considerations start with a given state ϱ_{AB} , so that it is clear that the assemblage of steering outcomes can be generated by a suitable set of measurements on Alice's side. In general, any non-signalling assemblage can be realised by suitable measurements on a suitable state [35–37].

For convenience, we will also consider Alice's Bloch hyperplane, $\mathcal{P}_A = \{X \in B^H(\mathcal{H}_A) : \text{Tr}(X) = 1\}$, and Alice's Bloch ball, $\mathcal{B}_A = \mathcal{P}_A \cap \mathcal{M}_A$. The boundary of Alice's Bloch ball is referred to as Alice's Bloch sphere, denoted by \mathcal{S}_A . The same notations with super/subscripts B apply to Bob's side.

In the Pauli coordinates, the positive cone is presented as the forward light cone at the origin. The set of measurement outcomes \mathcal{M}_A is a double cone, formed by intersecting the positive cone at 0 with the negative cone at $\mathbb{1}_A$; see Figure 2 (left) in the main text. The double cone \mathcal{M}_A has two vertices, 0 and $\mathbb{1}_A$, and an 'equator' of extreme points, which is the Bloch sphere \mathcal{S}_A .

Note that the steering outcome set $\Lambda(\mathcal{M}_A)$ is simply a linear image of \mathcal{M}_A , thus just a deformed double cone; see Figure 2 (right) in the main text. The set of steering outcomes has two vertices at 0 and $\varrho_B = \Lambda(\mathbb{1}_A)$. It also has an equator which is the image of the Bloch sphere $\Lambda(\mathcal{S}_A)$. Being a linear image of \mathcal{S}_A , this equator is in fact an ellipsoid if Λ is non-degenerate.

Appendix C: The capacity of an LHS ensemble

An LHS ensemble μ is a probability measure on Bob's Bloch ball. For a LHS ensemble, we define its capacity as the set of conditional states that Alice can simulate,

$$\mathcal{K}(\mu) = \left\{ K = \int d\mu(\sigma)g(\sigma)\sigma : 0 \leq g(\sigma) \leq 1 \right\}. \quad (\text{C1})$$

Note that for the case of two qubits this simplified capacity is sufficient for studying steering with projective measurement and with positive operator valued measures of 2 outcomes (2-POVM) as well since they are equivalent. For steering with more general POVMs or steering of systems in higher dimension, one would need the concept of n -capacity of μ ; see Ref. [27] for more details.

Now it is clear that a state ϱ is unsteerable with 2-POVMs (hereafter always considered from A to B , unless stated otherwise) if and only if there exists an LHS ensemble μ such that $\Lambda(\mathcal{M}_A) \subseteq \mathcal{K}(\mu)$ [20, 22, 27].

Appendix D: The minimal requirement and the principal radius

Fixing a choice of LHS ensemble μ , we can find an easy criterion for this nesting problem. Indeed, for $\mathcal{K}(\mu)$ to contain $\Lambda(\mathcal{M}_A)$, it is sufficient for it to contain all extreme points of $\Lambda(\mathcal{M}_A)$. If we impose the *minimal requirement* for the LHS ensemble

$$\varrho_B = \int d\mu(\sigma)\sigma, \quad (\text{D1})$$

then two vertices 0 and ϱ_B are automatically contained in $\mathcal{K}(\mu)$.

As described in the main text, it is left to check the inclusion in $\mathcal{K}(\mu)$ of the equator of the steering outcomes $\Lambda(\mathcal{S}_A)$. Recall that Λ is assumed to be invertible, so instead of working in Bob's space as described in the main text we can reverse the transformation to work in Alice's space; see Figure 6. More precisely, the inclusion of $\Lambda(\mathcal{S}_A)$ in $\mathcal{K}(\mu)$ is equivalent to the condition $\mathcal{S}_A \subseteq \Lambda^{-1}[\mathcal{K}(\mu)]$. The principal radius $r[\varrho, \mu]$ is then the minimal distance (in the normal Euclidean metric) from the centre of the Bloch sphere to the boundary of $\Lambda^{-1}[\mathcal{K}(\mu)]$ constrained to the Bloch hyperplane. Then $\mathcal{S}_A \subseteq \Lambda^{-1}[\mathcal{K}(\mu)]$ if and only if $r[\varrho, \mu] \geq 1$.

Appendix E: A simple formula for the critical radius of two qubits

In this section, with geometrical description of the principal radius above as the starting point, we give a proof for the formula equation (7) in the main text for the principal radius.

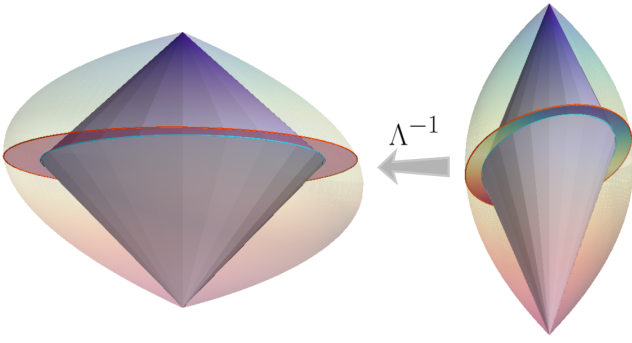


FIG. 6. Schematic representation of a capacity $\mathcal{K}(\mu)$ that contains the set of steering outcomes in Bob's space (left) and their images in Alice's space (right) via the action of Λ^{-1} .

Theorem 1. For a given (non-degenerate) state ϱ and for a given LHS ensemble μ satisfying the minimal requirement, $\varrho_B = \int d\mu(\sigma)\sigma$, the principal radius is given by

$$r[\varrho, \mu] = \inf_C \frac{\int d\mu(\sigma) |\text{Tr}(C\sigma)|}{\sqrt{2} \|\text{Tr}_B[\bar{\varrho}(\mathbb{1}_A \otimes C)]\|} \quad (\text{E1})$$

where $\bar{\varrho} = \varrho - \frac{\mathbb{1}_A}{2} \otimes \varrho_B$ and the minimisation is taken over all operators C on Bob's space.

We refer to the function under the infimum (E1) as the *fraction function* (inspired by the gap function in Ref. [27]),

$$F[\varrho, \mu, C] = \frac{\int d\mu(\sigma) |\langle C, \sigma \rangle|}{\sqrt{2} \|\text{Tr}_B[\bar{\varrho}(\mathbb{1}_A \otimes C)]\|}, \quad (\text{E2})$$

where we also use the Hilbert-Schmidt product notation $\langle C, \sigma \rangle = \text{Tr}(C\sigma)$. The fraction function is defined with the *denominator-dominated* convention, namely it is $+\infty$ whenever the denominator vanishes, regardless of the numerator. Using the Pauli basis defined in equation (A3), Section A, we represent operators by 4-vectors, $C \equiv \begin{pmatrix} c_0 \\ \mathbf{c} \end{pmatrix}$, $\sigma \equiv \begin{pmatrix} 1 \\ \mathbf{v} \end{pmatrix}$, and the bipartite state ρ by its Pauli tensor, $\rho \equiv \begin{pmatrix} 1 & \mathbf{b}^T \\ \mathbf{a} & T \end{pmatrix}$. In these coordinates, the fraction function can be written expressively,

$$F[\varrho, \mu, C] = \frac{\int d\mu(\mathbf{v}) |c_0 + \mathbf{c}^T \mathbf{v}|}{\|c_0 \mathbf{a} + T \mathbf{c}\|}, \quad (\text{E3})$$

where \mathbf{v} runs over vectors in Bob's Bloch ball. Being explicit, this formula is very convenient for direct computation. We will refer to both definitions (E2) and (E3) interchangeably.

Proof. To derive the formula (E1), we proceed as follows. As $\mathcal{K}(\mu)$ is a compact convex object in the 4D space of Bob's operators, we can define it by a set of linear inequalities, which are easy to determine. Transforming

it back to Alice's operator space, we obtain a set of inequalities that define $\Lambda^{-1}[\mathcal{K}(\mu)]$. Constraining this set of inequalities to the Bloch hyperplane $x_0 = 1$, we obtain a set of inequalities that define the cross-section of $\Lambda^{-1}[\mathcal{K}(\mu)]$ at $x_0 = 1$. Note that each inequality in this set corresponds to a 3D half-space, and the principal radius as described in Section D is simply the minimal distance from the corresponding separating 2D planes to the origin.

We start with finding the set of inequalities that define $\mathcal{K}(\mu)$. These inequalities can be found rather easily [20, 27]. Let Y be a point in the set $\mathcal{K}(\mu)$, then for any operator C

$$\langle C, Y \rangle \leq \max_{K \in \mathcal{K}(\mu)} \langle C, K \rangle. \quad (\text{E4})$$

The left-hand side can be solved rather easily,

$$\begin{aligned} \max_{K \in \mathcal{K}(\mu)} \langle C, K \rangle &= \max_{0 \leq g(\sigma) \leq 1} \int d\mu(\sigma) g(\sigma) \langle C, \sigma \rangle \\ &= \int d\mu(\sigma) \max\{\langle C, \sigma \rangle, 0\}. \end{aligned} \quad (\text{E5})$$

This should be viewed as a family in inequalities parametrised by C that defines $\mathcal{K}(\mu)$.

The inequalities that define $\Lambda^{-1}[\mathcal{K}(\mu)]$ can be found by replacing the operator $Y \in \mathcal{K}(\mu)$ by $Y = \Lambda(X)$ for $X \in \Lambda^{-1}[\mathcal{K}(\mu)]$ in (E4). Using the explicit coordinates, $C \equiv \begin{pmatrix} c_0 \\ \mathbf{c} \end{pmatrix}$, $\sigma \equiv \begin{pmatrix} 1 \\ \mathbf{v} \end{pmatrix}$, $X \equiv \begin{pmatrix} x_0 \\ \mathbf{x} \end{pmatrix}$, $\Lambda \equiv \frac{1}{2} \begin{pmatrix} 1 & \mathbf{a}^T \\ \mathbf{b} & T^T \end{pmatrix}$, these inequalities can be written as

$$\frac{1}{2} (c_0 \ \mathbf{c}^T) \begin{pmatrix} 1 & \mathbf{a}^T \\ \mathbf{b} & T^T \end{pmatrix} \begin{pmatrix} x_0 \\ \mathbf{x} \end{pmatrix} \leq \int d\mu(\mathbf{v}) \max\{c_0 + \mathbf{c}^T \mathbf{v}, 0\}. \quad (\text{E6})$$

More explicitly, we have

$$(c_0 \mathbf{a}^T + \mathbf{c}^T T^T) \mathbf{x} \leq 2 \int d\mu(\mathbf{v}) \max\{c_0 + \mathbf{c}^T \mathbf{v}, 0\} - x_0 (c_0 + \mathbf{c}^T \mathbf{b}). \quad (\text{E7})$$

This should be viewed as a family of inequalities parametrised by (c_0, \mathbf{c}) that defines $\Lambda^{-1}[\mathcal{K}(\mu)]$ consisting of points $X \equiv \begin{pmatrix} x_0 \\ \mathbf{x} \end{pmatrix}$.

To check if $\Lambda^{-1}[\mathcal{K}(\mu)]$ contains \mathcal{M}_A , we only need to check the condition at the equator \mathcal{S}_A (since μ satisfies the minimal requirement). Since \mathcal{S}_A belongs to the Bloch hyperplane \mathcal{P}_A , we can fix $x_0 = 1$ and (E7) becomes

$$(c_0 \mathbf{a}^T + \mathbf{c}^T T^T) \mathbf{x} \leq \int d\mu(\mathbf{v}) |c_0 + \mathbf{c}^T \mathbf{v}|, \quad (\text{E8})$$

where we have also used the minimal requirement $\mathbf{b} = \int d\mu(\mathbf{v}) \mathbf{v}$ to simplify the right-hand side. Then (E8) is a family of 3D half-spaces with normal vectors $(c_0 \mathbf{a}^T + \mathbf{c}^T T^T)$ and offsets $\int d\mu(\mathbf{v}) |c_0 + \mathbf{c}^T \mathbf{v}|$. The distance of each of the separating planes to the origin is

$$\frac{\int d\mu(\mathbf{v}) |c_0 + \mathbf{c}^T \mathbf{v}|}{\|c_0 \mathbf{a} + T \mathbf{c}\|}. \quad (\text{E9})$$

By definition,

$$r[\varrho, \mu] = \inf_{c_0, \mathbf{c}} \frac{\int d\mu(\mathbf{v}) |c_0 + \mathbf{c}^T \mathbf{v}|}{\|c_0 \mathbf{a} + T\mathbf{c}\|}. \quad (\text{E10})$$

This is precisely the formula for the principal radius in the coordinate form equation (E3). \square

Appendix F: Relaxing the non-degeneracy condition of the state

Strictly, the definition for the principal radius applies only to non-degenerate states. One however can take equation (E1) as the primary definition of the principal radius, which works also for degenerate states. The above proof can be easily adapted to show that a state is unsteerable with a specific choice of LHS ensemble μ if and only if $r[\varrho, \mu] \geq 1$ with the principal radius as defined by equation (E1).

Appendix G: Defining domain of the principal radius

From the formula (E1), one can easily see that the principal radius is well-defined even when ϱ is not a proper state. In the following, when referring to a *state*, we do not impose positivity on it. When imposing positivity on a state, we refer to it as a *proper state*.

For the principal radius to be well-defined, it is prerequisite that ϱ_B is inside Bob's Bloch ball. This is to guarantee that the minimal requirement does not result in an empty-set of probability measures. It is easy to see that the set of states that have Bob's reduced states inside Bob's Bloch ball is convex and closed. This set is the (most general) defining domain we consider.

Appendix H: Concavity of the principal radius

Proposition 2. *The principal radius $r[\varrho, \mu]$ is concave in μ .*

Proof. Since $r[\varrho, \mu]$ is an infimum of a family of linear, thus concave, functions in μ , $r[\varrho, \mu]$ must be itself concave in μ . \square

Although not mandatory in the following, it is worth noting that the convexity of $r^{-1}[\varrho, \mu]$ is somewhat better behaved.

Proposition 3. *The inverse principal radius $r^{-1}[\varrho, \mu]$ is convex either in μ or ϱ , if ϱ is constrained by $\text{Tr}_A[\varrho] = \varrho_B$.*

Proof. The convexity in ϱ is limited to decompositions which respect the (affine) constraint $\text{Tr}_A[\varrho] = \varrho_B$ (so that

μ satisfies the minimal requirement for all states under consideration). We write

$$r^{-1}[\varrho, \mu] = \sup_C \frac{\sqrt{2} \|\bar{\varrho}(\mathbb{1}_A \otimes C)\|}{\int d\mu(P) |\langle C, P \rangle|}. \quad (\text{H1})$$

Now the function under the supremum is convex either in μ or ϱ . Therefore $r^{-1}[\varrho, \mu]$ is convex either in μ or ϱ . \square

Appendix I: Upper-semicontinuity of the principal radius

To study in detail the topological properties of the principal radius, we need a weaker notion of continuity, namely semicontinuity.

Recall that $\bar{\mathbb{R}} = \mathbb{R} \cup \{-\infty\} \cup \{+\infty\}$. Consider a sequence $\{u_n\}_{n=1}^{+\infty}$ in $\bar{\mathbb{R}}$. The limit of a subsequence of $\{u_n\}$ is called an accumulation point. The set of accumulation points is closed; its maximum is called the limit superior of $\{u_n\}$, denoted by $\overline{\lim}_{n \rightarrow \infty} u_n$, and the minimum is called the limit inferior of $\{u_n\}$, denoted by $\underline{\lim}_{n \rightarrow \infty} u_n$.

Below we assume that X is a metric space.

A function $f : X \rightarrow \bar{\mathbb{R}}$ is said to be upper-semicontinuous at $x \in X$ if for any sequence $\{x_n\} \rightarrow x$, one has $\overline{\lim}_{n \rightarrow \infty} f(x_n) \leq f(x)$. An upper-semicontinuous function on a compact metric space attains its maximum.

Similarly, a function $f : X \rightarrow \bar{\mathbb{R}}$ is said to be lower-semicontinuous at $x \in X$ if for any sequence $\{x_n\} \rightarrow x$, one has $\underline{\lim}_{n \rightarrow \infty} f(x_n) \geq f(x)$. A lower-semicontinuous function on a compact metric space attains its minimum.

A function $f : X \rightarrow \bar{\mathbb{R}}$ is continuous at $x \in X$ if and only if it is both upper-semicontinuous and lower-semicontinuous at x .

To study the upper-semicontinuity of $r[\varrho, \mu]$, we need the following lemma.

Lemma 4. *Consider $f : X \times Y \rightarrow \bar{\mathbb{R}}$ where X is a metric space and Y is an arbitrary set. Define $g : X \rightarrow \bar{\mathbb{R}}$ by $g(x) = \inf_{y \in Y} f(x, y)$. Suppose all the functions $f(\cdot, y) : X \rightarrow \bar{\mathbb{R}}$ with $y \in Y$ are upper-semicontinuous at a certain x , then g is upper-semicontinuous at x .*

Proof. We would like to show that for any converging sequence $\{x_n\} \rightarrow x$, we have

$$\overline{\lim}_{n \rightarrow \infty} g(x_n) \leq g(x). \quad (\text{I1})$$

Because $g(x) = \inf_{y \in Y} f(x, y)$, there exists $y_0 \in Y$ such that

$$f(x, y_0) \leq g(x). \quad (\text{I2})$$

Now because for all x_n ,

$$g(x_n) = \inf_{y \in Y} f(x_n, y) \leq f(x_n, y_0), \quad (\text{I3})$$

we have that

$$\overline{\lim}_{n \rightarrow \infty} g(x_n) \leq \overline{\lim}_{n \rightarrow \infty} f(x_n, y_0). \quad (\text{I4})$$

And because $f(\cdot, y_0)$ is upper-semicontinuous at x ,

$$\overline{\lim}_{n \rightarrow \infty} f(x_n, y_0) \leq f(x, y_0) \leq g(x). \quad (\text{I5})$$

So we indeed have (I1). \square

The space of probabilistic Borel measures over the Bloch sphere is metrizable and weakly compact; see, e.g., Ref. [38, Theorem 6.3.5, 7.2.2, 8.3.2, 8.9.3, 8.9.4]. Then its intersection with the minimal constraint (which is weakly closed) is also metrizable and weakly compact. From Theorem 1 and Lemma 4, we can then easily prove the following proposition.

Proposition 5. *The principal radius $r[\varrho, \mu]$ is weakly upper-semicontinuous in μ .*

Proof. It is easy to check that for fixed C , the fraction function $F[\varrho, \mu, C]$ in equation (E2) is upper-semicontinuous in μ with respect to the weak topology. To be more precise, for all C such that $\|\bar{\varrho}(\mathbb{1}_A \otimes C)\| \neq 0$, $F[\varrho, \mu, C]$ is continuous in μ . For $\|\bar{\varrho}(\mathbb{1}_A \otimes C)\| = 0$, $F[\varrho, \mu, C]$ is $+\infty$, thus trivially upper-semicontinuous. Therefore $r[\varrho, \mu]$ is weakly upper-semicontinuous as a consequence of Lemma 4. \square

In contrast to upper-semicontinuity, the lower-semicontinuity of the principal radius is rather subtle. We postpone this study until we have discussed the canonical form of a state; see Section P.

Appendix J: Existence of an optimal LHS ensemble

As the principal radius $r[\varrho, \mu]$ is upper-semicontinuous over the compact space of probabilistic Borel measures μ satisfying the minimal requirement, it attains its maximum. The critical radius of ϱ is then defined by

$$R[\varrho] = \max_{\mu} r[\varrho, \mu], \quad (\text{J1})$$

where the maximum is taken over probabilistic Borel measures satisfying the minimal requirement (D1). Physically, we have proved the following statement:

Theorem 6 (Existence of optimal LHS ensemble). *For any two-qubit state ϱ , there exists an optimal LHS ensemble for steering given by $\mu^* = \arg \max r[\varrho, \mu]$.*

Note that this concept of optimal LHS ensemble is similar (but not identical) to that of optimal LHS model defined in the original paper by Wiseman *et al.* [5]. There, an optimal LHS model consists of an LHS ensemble and a choice of response functions which is also optimal in a certain sense. It is still unknown whether or not one can construct optimal response functions. Here we prove that an optimal choice of LHS ensemble does exist. The existence of an optimal LHS ensemble changes the perspective on the problem of determining the steerability of a state. Now, instead of checking every LHS ensemble, we search for a specific LHS ensemble. Moreover,

instead of checking all possible choices of response functions, the single value of the critical radius is enough to tell about the steerability of the state. All is then about how to compute the critical radius. We discuss the practical computation of the critical radius in Section U.

Appendix K: Implication of symmetry on the optimal LHS ensemble

We say a state ϱ is (\mathcal{G}, U, V) -symmetric with a compact group \mathcal{G} with its two actions U on \mathcal{H}_A and V on \mathcal{H}_B if $U(g) \otimes V(g) \varrho U^\dagger(g) \otimes V^\dagger(g)$ for all $g \in \mathcal{G}$. Recall that the action V on \mathcal{H}_B induces an action on the measures on \mathcal{B}_B , defined by $R_V(g)[\mu](X) = \mu[V(g)XV^\dagger(g)]$ for all measurable subsets X of \mathcal{B}_B .

Theorem 7 (Symmetry of LHS ensemble). *If ϱ is (\mathcal{G}, U, V) -symmetric, then there exists an optimal ensemble μ^* which is (\mathcal{G}, V) -invariant, $R_V(g)[\mu^*] = \mu^*$.*

Proof. This theorem is a simple consequence of the concavity of $r[\varrho, \mu]$ in μ . We will only sketch the proof. Let μ^* be an optimal LHS ensemble for ϱ , namely, $R[\varrho] = r[\varrho, \mu^*]$. From the formula of the principal radius, and with the symmetry of ϱ , one can easily verify that also $r[\varrho, R_V(g)[\mu^*]] = R[\varrho]$. Define a measure $\bar{\mu}^*$ on \mathcal{B}_B by $\bar{\mu}^* = \int d\omega(g) R_V(g)[\mu^*]$, where ω is the Haar measure of \mathcal{G} . It is easy to see that $\bar{\mu}^*$ is invariant under \mathcal{G} . We show that it is an optimal LHS ensemble. Due to the concavity of $r[\varrho, \mu]$ in μ , we have $r[\varrho, \bar{\mu}^*] \geq \int d\omega(g) r[\varrho, R_V(g)[\mu^*]] = R[\varrho]$. On the other hand, by the definition of the critical radius, $r[\varrho, \bar{\mu}^*] \leq R[\varrho]$. We therefore have $r[\varrho, \bar{\mu}^*] = R[\varrho]$, or $\bar{\mu}^*$ is an optimal LHS ensemble. \square

One may observe from the above proof that the symmetry of LHS ensembles is determined only by the action V (and not U). In fact, the notion of the (\mathcal{G}, U, V) -symmetric state seems a bit stronger than necessary. This is indeed the case. In fact, the theorem can be formulated as: when the set of steering outcomes $\Lambda(\mathcal{M}_A)$ is (\mathcal{G}, V) -symmetric, then LHS ensembles can be assumed to be (\mathcal{G}, V) -symmetric.

Appendix L: Scaling of the critical radius

Theorem 8 (Scaling of the critical radius). *For any state ϱ and any $\lambda \geq 0$, we have*

$$R[\varrho] = \lambda R[\lambda\varrho + (1-\lambda)\frac{\mathbb{1}_A}{2} \otimes \varrho_B]. \quad (\text{L1})$$

Note that the theorem applies as well if $\lambda\varrho + (1-\lambda)\frac{\mathbb{1}_A}{2} \otimes \varrho_B$ is not a proper state.

Proof. The proof is trivial given formula (E1). One simply inserts $\lambda\varrho + (1-\lambda)\frac{\mathbb{1}_A}{2} \otimes \varrho_B$ to find that $r[\lambda\varrho + (1-\lambda)\frac{\mathbb{1}_A}{2} \otimes \varrho_B, \mu] = \frac{1}{\lambda} r[\varrho, \mu]$, which implies equation (L1). \square

Note that by setting $\lambda = 0$, we find $R[\frac{\mathbb{1}_A}{2} \otimes \varrho_B] = +\infty$. Thus the critical radius can be infinite; we will see below that it is infinite only at states of this form. Geometrically, along the scaling line, the equator of the steering outcomes $\Lambda(\mathcal{S}_A)$ is uniformly rescaled by the factor λ . At $\lambda = 0$, the equator degenerates to a single point.

Appendix M: Continuous symmetry of the critical radius

The Bloch hyperplane for two qubits, denoted by \mathcal{P} , is the linear manifold of hermitian trace-1 operators acting on $\mathcal{H}_A \otimes \mathcal{H}_B$. For $U \in \text{U}(2)$, $V \in \text{GL}(2)$, consider the affine transformation from the Bloch hyperplane of the joint system into itself $\varphi_{(U,V)} : \mathcal{P} \rightarrow \mathcal{P}$, defined by

$$\varphi_{(U,V)}(X) = \frac{(U \otimes V)X(U^\dagger \otimes V^\dagger)}{\text{Tr}[(U \otimes V)X(U^\dagger \otimes V^\dagger)]}. \quad (\text{M1})$$

for $X \in \mathcal{P}$. Note that this is a group action of $\text{U}(2) \times \text{GL}(2)$ on \mathcal{P} . Moreover $\varphi_{(U,V)}$ conserves the positivity, thus also maps the set of (bipartite) proper states into itself.

Accepting a bit of ambiguity in notation for the sake of simplicity, for $V \in \text{GL}(2)$, we also denote $\varphi_V : \mathcal{B}_B \rightarrow \mathcal{B}_B$ defined by

$$\varphi_V(\sigma) = \frac{V\sigma V^\dagger}{\text{Tr}(V\sigma V^\dagger)}. \quad (\text{M2})$$

Lemma 9. *Consider a given state ϱ and a given probability measure (LHS ensemble) μ satisfying the minimal requirement $\int d\mu(\sigma)\sigma = \varrho_B$. For $U \in \text{U}(2)$ and $V \in \text{GL}(2)$, we denote $\tilde{\varrho} = \varphi_{(U,V)}(\varrho)$. Note that there exists a unique probability measure $\tilde{\mu}$ on \mathcal{B}_B defined by*

$$\int d\tilde{\mu}(\sigma)f(\sigma) = \frac{1}{\text{Tr}(V\varrho_B V^\dagger)} \int \frac{d\mu \circ \varphi_{V^{-1}}(\sigma)}{\text{Tr}[V^{-1}\sigma(V^{-1})^\dagger]} f(\sigma) \quad (\text{M3})$$

for all continuous functions f . Then $\tilde{\mu}$ satisfies the minimal requirement for $\tilde{\varrho}$ and $r[\varrho, \mu] = r[\tilde{\varrho}, \tilde{\mu}]$.

Proof. (i) To prove that $\tilde{\mu}$ satisfies the minimal requirement for $\tilde{\varrho}$, we need to show that

$$\frac{V\varrho_B V^\dagger}{\text{Tr}(V\varrho_B V^\dagger)} = \int d\tilde{\mu}(\sigma)\sigma. \quad (\text{M4})$$

Using the definition of $\tilde{\mu}$, we have

$$\int d\tilde{\mu}(\sigma)\sigma = \frac{1}{\text{Tr}(V\varrho_B V^\dagger)} \int \frac{d\mu \circ \varphi_{V^{-1}}(\sigma)}{\text{Tr}[V^{-1}\sigma(V^{-1})^\dagger]} \sigma. \quad (\text{M5})$$

By changing the variable of integral, $\sigma = \varphi_V(\tau)$,

$$\begin{aligned} \int \frac{d\mu \circ \varphi_{V^{-1}}(\sigma)}{\text{Tr}[V^{-1}\sigma(V^{-1})^\dagger]} \sigma &= \int d\mu(\tau) \frac{\varphi_V(\tau)}{\text{Tr}[V^{-1}\varphi_V(\tau)(V^{-1})^\dagger]} \\ &= \int d\mu(\tau) V\tau V^\dagger \\ &= V\varrho_B V^\dagger, \end{aligned} \quad (\text{M6})$$

where we have used the minimal requirement for μ , $\int d\mu(\tau)\tau = \varrho_B$. From (M6) and (M5), we obtain (M4).

(ii) Now we prove that $r[\varrho, \mu] = r[\tilde{\varrho}, \tilde{\mu}]$. Using the definition (E1), we have $r[\tilde{\varrho}, \tilde{\mu}]$ as

$$\inf_C \frac{1}{\sqrt{2} \|\text{Tr}_B[\tilde{\varrho}(\mathbb{1}_A \otimes C)]\| \text{Tr}(V\varrho_B V^\dagger)} \int \frac{d\mu \circ \varphi_V^{-1}(\sigma) |\langle C, \sigma \rangle|}{\text{Tr}(V^{-1}\sigma(V^{-1})^\dagger)}, \quad (\text{M7})$$

where $\tilde{\varrho} = \tilde{\varrho} - \frac{\mathbb{1}_A}{2} \otimes \varrho_B$. In the numerator, we make a change of the integration variable $\sigma = \varphi_V(\tau)$,

$$\begin{aligned} \int \frac{d\mu \circ \varphi_V^{-1}(\sigma) |\langle C, \sigma \rangle|}{\text{Tr}(V\sigma V^\dagger)} &= \int \frac{d\mu(\tau) |\langle C, \varphi_V(\tau) \rangle|}{\text{Tr}(V^{-1}\varphi_V(\tau)(V^{-1})^\dagger)} \\ &= \int \mu(\tau) |\langle V^\dagger C V, \tau \rangle|. \end{aligned} \quad (\text{M8})$$

In the denominator, we have

$$\begin{aligned} \text{Tr}_B[\tilde{\varrho}(\mathbb{1}_A \otimes C)] &= \frac{\text{Tr}_B[(U \otimes V)\tilde{\varrho}(U^\dagger \otimes V^\dagger)(\mathbb{1}_A \otimes C)]}{\text{Tr}(V\varrho_B V^\dagger)} \\ &= \frac{\text{Tr}_B[\tilde{\varrho}(\mathbb{1}_A \otimes V^\dagger C V)]}{\text{Tr}(V\varrho_B V^\dagger)}. \end{aligned} \quad (\text{M9})$$

So we have

$$\begin{aligned} r[\tilde{\varrho}, \tilde{\mu}] &= \inf_C \frac{\int d\mu(\sigma) |\langle V^\dagger C V, \sigma \rangle|}{\sqrt{2} \|\text{Tr}_B[\tilde{\varrho}(\mathbb{1}_A \otimes V^\dagger C V)]\|} \\ &= \inf_C \frac{\int d\mu(\sigma) |\langle C, \sigma \rangle|}{\sqrt{2} \|\text{Tr}_B[\tilde{\varrho}(\mathbb{1}_A \otimes C)]\|}, \end{aligned} \quad (\text{M10})$$

where we have used the fact that $C \mapsto VCV^\dagger$ is bijective. The last expression then coincides with $r[\varrho, \mu]$. \square

The invariance of the principal radius also has a simple geometrical interpretation. Under the local unitary transformation U on Alice's side, the set of steering outcomes $\Lambda(\mathcal{M}_A)$ is invariant. On the other hand, under the (so-called) local filtering V on Bob's side, $\Lambda(\mathcal{M}_A)$ and $\mathcal{K}(\mu)$ transform covariantly; depending only on the relative geometry of $\Lambda(\mathcal{M}_A)$ and $\mathcal{K}(\mu)$, the principal radius is invariant.

Theorem 10 (Continuous symmetry of the critical radius). *For any state ϱ and $U \in \text{U}(2)$, $V \in \text{GL}(2)$, we have $R[\varrho] = R[\varphi_{(U,V)}\varrho]$.*

Proof. Let μ^* be an optimal LHS ensemble for ϱ , then $R[\varrho] = r[\varrho, \mu^*]$. Let $\tilde{\mu}^*$ be defined as in Lemma 9, then $r[\varrho, \mu^*] = r[\tilde{\varrho}, \tilde{\mu}^*] \leq R[\tilde{\varrho}]$, thus $R[\varrho] \leq R[\tilde{\varrho}]$. Applying the Lemma for the reversed transformation from $\tilde{\varrho}$ to ϱ , we find $R[\tilde{\varrho}] \leq R[\varrho]$. It then follows that $R[\varrho] = R[\tilde{\varrho}]$. \square

Appendix N: Time-reversal symmetry of the critical radius

Consider Alice's Bloch hyperplane \mathcal{P}_A and fix the Pauli basis. The time-reversal transformation on Alice's

Bloch hyperplane is the transformation $T_A : \mathcal{P}_A \rightarrow \mathcal{P}_A$, $X \mapsto T_A(X) = X^*$, where X^* is the complex conjugation of X . Geometrically, T_A is the reflection along σ_y . Therefore T_A maps Alice's Bloch ball to itself. Upto a unitary transformation, T_A is also equivalent to the inversion of \mathcal{P}_A through $\frac{\mathbb{1}_A}{2}$. In fact, we will not distinguish different implementations of the time-reversal transformation which are equivalent upto some unitary transformations.

On a bipartite state ϱ , T_A is extended to partial time-reversal transformation $T_A \otimes \mathcal{J}_B$, where \mathcal{J}_B is the identity map on Bob's space. The same notation is applied to the time-reversal transformation on Bob's side. Upto local unitary transformations, the partial time-reversal transformation is equivalent to the partial transposition. Note that on the bipartite Bloch hyperplane, $T_A \otimes \mathcal{J}_B$ does not map the set of *proper* states into itself. In fact, the subset of proper states that is invariant under $T_A \otimes \mathcal{J}_B$ are separable states—by the Peres–Horodecki criterion of the partial transposition [31, 32]. Somehow unexpectedly, for steerability, the following theorem tells that the critical radius R is invariant under the partial time-reversal transformations.

Theorem 11 (Time-reversal symmetry of the critical radius). *For any state ϱ , we have $R[\varrho] = R[(T_A \otimes \mathcal{J}_B)\varrho] = R[(\mathcal{J}_A \otimes T_B)\varrho]$.*

While quantum steering is asymmetric between two parties, this theorem has a rather symmetric form between the time-reversals on either of the parties. The proof, however, seems to suggest that this symmetry is perhaps rather accidental.

Proof. (i) We start with proving $R[\varrho] = R[(T_A \otimes \mathcal{J}_B)\varrho]$. In fact we can show the *invariance* of the principal radius, $r[\varrho, \mu] = r[(T_A \otimes \mathcal{J}_B)\varrho, \mu]$. This is easily seen because the numerator of (E1) is invariant under the transformation, the denominator is also invariant since the time-reversal is isometric.

(ii) The proof that $R[\varrho] = R[(\mathcal{J}_A \otimes T_B)\varrho]$ is only slightly different. It follows from the *covariance* of the principal radius, $r[\varrho, \mu] = r[(\mathcal{J}_A \otimes T_B)\varrho, \mu \circ T_B^{-1}]$. Clearly the minimal requirement is covariant, namely,

$$T_B(\varrho_B) = \int d\mu \circ T_B^{-1}(\sigma)\sigma. \quad (\text{N1})$$

Moreover, we have

$$r[(\mathcal{J}_B \otimes T_B)\varrho, \mu \circ T_B^{-1}] = \inf_C \frac{\int d\mu \circ T_B^{-1}(\sigma) |\langle C, \sigma \rangle|}{\sqrt{2} \|\text{Tr}_B[(\mathcal{J}_A \otimes T_B)\bar{\varrho}(\mathbb{1}_A \otimes C)]\|}, \quad (\text{N2})$$

where $\bar{\varrho} = \varrho - \frac{\mathbb{1}_A}{2} \otimes \varrho_B$. Now we note that T_B is symmetric on the hermitian operators, $\langle X, T_B(Y) \rangle = \langle T_B(X), Y \rangle$. In the numerator, changing the integration variable and applying the symmetry of T_B , we arrive at

$$\int d\mu \circ T_B^{-1}(\sigma) |\langle C, \sigma \rangle| = \int d\mu(\sigma) |\langle T_B(C), \sigma \rangle|. \quad (\text{N3})$$

In the denominator, we have the identity

$$\text{Tr}_B[(\mathcal{J}_A \otimes T_B)\bar{\varrho}(\mathbb{1}_A \otimes C)] = \text{Tr}_B[\bar{\varrho}(\mathbb{1}_A \otimes T_B(C))], \quad (\text{N4})$$

which can be proved by expanding $\bar{\varrho}$ in product operators and verifying it for every product operator term. Collecting both the numerator and the denominator, we then have

$$r[(\mathcal{J}_B \otimes T_B)\varrho, \mu \circ T_B^{-1}] = \inf_C \frac{\int d\mu(\sigma) |\langle T_B(C), \sigma \rangle|}{\sqrt{2} \|\text{Tr}_B[\bar{\varrho}(\mathbb{1}_A \otimes T_B(C))]\|}, \quad (\text{N5})$$

which is expressively the same as $r[\varrho, \mu]$ since T_B is bijective. \square

From the above proof, one may find a similar geometrical signature as the continuous symmetry of the critical radius: the local time-reversal transformation on Alice's space leaves $\Lambda(\mathcal{M}_A)$ invariant, while the local time-reversal transformation on Bob's side acts covariantly on $\Lambda(\mathcal{M}_A)$ and $\mathcal{K}(\mu)$.

Appendix O: The canonical form and normal states

A generic state is fully characterised by Alice's and Bob's Bloch vectors \mathbf{a} and \mathbf{b} and their correlation matrix T . We therefore sometimes identify ϱ with a triple $(\mathbf{a}, T, \mathbf{b})$, $\varrho \equiv (\mathbf{a}, T, \mathbf{b})$.

If Bob's reduced state is pure, the bipartite state is called *abnormal*. In this case, there exists only a single measure that satisfies the minimal requirement, namely the one supported only at Bob's reduced state. The critical radius then reads,

$$R[(\mathbf{a}, T, \mathbf{b})] = \inf_{c_0, \mathbf{c}} \frac{|c_0 + \mathbf{c}^T \mathbf{b}|}{\|c_0 \mathbf{a} + T \mathbf{c}\|}, \quad (\text{O1})$$

where we have used the Bloch parameters \mathbf{a} , \mathbf{b} , T to denote the state. To find this infimum, we change the variable $c'_0 = c_0 + \mathbf{c}^T \mathbf{b}$ and have

$$R[(\mathbf{a}, T, \mathbf{b})] = \inf_{c'_0, \mathbf{c}} \frac{|c'_0|}{\|c'_0 \mathbf{a} + (T - \mathbf{a} \mathbf{b}^T) \mathbf{c}\|}. \quad (\text{O2})$$

One then finds that for abnormal states, we have

$$R[(\mathbf{a}, T, \mathbf{b})] = \begin{cases} \frac{1}{\|\mathbf{a}\|} & \text{if } T = \mathbf{a} \mathbf{b}^T \text{ (product states),} \\ 0 & \text{if } T \neq \mathbf{a} \mathbf{b}^T. \end{cases} \quad (\text{O3})$$

Note that if the abnormal state is a proper state (i.e., positive), it must be a product state and thus unsteerable.

If Bob's reduced state is not pure, the state is said to be *normal*. By the continuous symmetry of the critical radius Theorem 10, a normal state can always be brought into the *canonical form* without changing the critical radius,

$$\Theta = \begin{pmatrix} 1 & \mathbf{0}^T \\ \mathbf{a} & T \end{pmatrix}, \quad (\text{O4})$$

where \mathbf{a} is Alice's reduced state, and T is the correlation matrix, which can also be assumed to be diagonal $T = \text{diag}(\mathbf{s})$. Note that the canonical parameters, that is, its Alice's reduced state and the correlation diagonal in the canonical form, vary continuously as functions of ϱ limited to the set of normal states. Moreover if a normal states is non-degenerate, its canonical form is also non-degenerate (and vice versa).

For a state in the canonical form, we also identify the notation $\varrho \equiv (\mathbf{a}, T)$. In fact, the importance of the canonical form to studying quantum steering cannot be over-emphasised. Let us note immediately some interesting properties of the canonical form.

First, for canonical states, the invariance of the critical radius under partial time-reversal transformation implies that $R[(\mathbf{a}, T)] = R[(-\mathbf{a}, -T)] = R[(\mathbf{a}, -T)] = R[(-\mathbf{a}, T)]$.

Second, the minimum requirement $\int d\mu(\mathbf{v})\mathbf{v} = 0$ is independent of the canonical state $\varrho = (\mathbf{a}, T)$. This is in fact a every important technical point, which renders studying of general properties of the critical radius such as its continuity possible at all.

And third, the operator C in the fraction function can be limited to some simple constraints:

Lemma 12. *For a two-qubit canonical state $\varrho = (\mathbf{a}, T)$, the critical radius can be found by*

$$r[\varrho, \mu] = \inf_{c_0, \mathbf{c}} \frac{\int d\mu(\mathbf{v})|c_0 + \mathbf{c}^T \mathbf{v}|}{\|c_0 \mathbf{a} + T \mathbf{c}\|}. \quad (\text{O5})$$

where c_0 and \mathbf{c} can be subjected to canonical constraints $\|\mathbf{c}\| = 1$ and $-1 \leq c_0 \leq +1$.

Proof. Let us recall the fraction function

$$F[\varrho, \mu, c_0, \mathbf{c}] = \frac{\int d\mu(\mathbf{v})|c_0 + \mathbf{c}^T \mathbf{v}|}{\|c_0 \mathbf{a} + T \mathbf{c}\|}. \quad (\text{O6})$$

We first note that we can assume $\mathbf{c} \neq 0$. This is because $F[\varrho, \mu, c_0, \mathbf{c} = 0] = \frac{1}{\|\mathbf{a}\|} \geq \lim_{c_0 \rightarrow \infty} F[\varrho, \mu, c_0, \mathbf{c} \neq 0] \geq \inf_{c_0, \mathbf{c} \neq 0} F[\varrho, \mu, c_0, \mathbf{c} \neq 0]$.

Now since for all $\lambda > 0$, $F[\varrho, \mu, c_0, \mathbf{c}] = F[\varrho, \mu, \lambda c_0, \lambda \mathbf{c}]$, we can out the constraint $\|\mathbf{c}\| = 1$ by choosing an appropriate λ .

We next show that $F[\varrho, \mu, c_0, \mathbf{c}]$ with $\|\mathbf{c}\| = 1$ and $|c_0| \geq 1$ attains the infimum at $|c_0| = 1$. To see this, note that for $\|\mathbf{c}\| = 1$ and $|c_0| \geq 1$, we have either $c_0 + \mathbf{c}^T \mathbf{v} \geq 0$ or $c_0 + \mathbf{c}^T \mathbf{v} \leq 0$ for all \mathbf{v} in Bob's Bloch ball. Therefore $\int d\mu(\mathbf{v})|c_0 + \mathbf{c}^T \mathbf{v}| = |\int d\mu(\mathbf{v})(c_0 + \mathbf{c}^T \mathbf{v})| = |c_0|$. Thus, for $\|\mathbf{c}\| = 1$ and $|c_0| \geq 1$, we have

$$F[\varrho, \mu, c_0, \mathbf{c}] = \frac{1}{\left\| \mathbf{a} + T \frac{\mathbf{c}}{c_0} \right\|}, \quad (\text{O7})$$

which clearly attains the infimum at $c_0 = \pm 1$.

To summarise, we therefore can limit the infimum in computing the principal radius from the fraction function to $\|\mathbf{c}\| = 1$ and $-1 \leq c_0 \leq 1$. \square

Appendix P: Lower-semicontinuity of the principal radius

For the sake of convenience, we will limit our analysis to non-degenerate states in the canonical form only. This is sufficient to decide steerability.

Lemma 13. *Consider $f : X \times Y \rightarrow \bar{\mathbb{R}}$ where X is a metric space and Y is a compact metric space. Define $g : X \rightarrow \bar{\mathbb{R}}$ by $g(x) = \inf_{y \in Y} f(x, y)$. Suppose at a certain x , the function f is jointly lower-semicontinuous at (x, y) for all $y \in Y$. Moreover suppose the function $f(x', \cdot) : Y \rightarrow \bar{\mathbb{R}}$ attains its infimum over Y for all x' in a neighbourhood $V(x)$ of x . Then g is lower-semicontinuous at x .*

Proof. We would like to show that for any converging sequence $\{x_n\} \rightarrow x$, we have

$$\underline{\lim}_{n \rightarrow \infty} g(x_n) \geq g(x). \quad (\text{P1})$$

Without loss of generality, we can assume that $x_n \in V(x)$ for all n .

Letting $\{x_k\}$ be a subsequence of $\{x_n\}$ such that $\{g(x_k)\}$ converges to $\underline{\lim}_{n \rightarrow \infty} g(x_n)$, we have

$$\lim_{k \rightarrow \infty} g(x_k) = \underline{\lim}_{n \rightarrow \infty} g(x_n). \quad (\text{P2})$$

Now because for every $x_k \in V(x)$, $g(x_k, \cdot)$ attains its infimum, there exists y_k such that

$$g(x_k) = f(x_k, y_k). \quad (\text{P3})$$

and thus in particular

$$\lim_{k \rightarrow \infty} g(x_k) = \lim_{k \rightarrow \infty} f(x_k, y_k). \quad (\text{P4})$$

Because Y is compact, there exists a subsequence $\{y_p\}$ of $\{y_k\}$ that converges to certain point y_0 of Y . We also have

$$\lim_{k \rightarrow \infty} g(x_k) = \lim_{p \rightarrow \infty} f(x_p, y_p). \quad (\text{P5})$$

Note that $\{(x_p, y_p)\} \rightarrow (x, y_0)$ and because f is jointly lower-semicontinuous at (x, y_0) by assumption, we have

$$\lim_{p \rightarrow \infty} f(x_p, y_p) \geq f(x, y_0). \quad (\text{P6})$$

On the other hand, $f(x, y_0) \geq g(x) = \inf_{y \in Y} f(x, y)$, thus

$$\lim_{p \rightarrow \infty} f(x_p, y_p) \geq g(x). \quad (\text{P7})$$

Then equation (P1) follows directly. \square

Corollary 14. *Consider $f : X \times Y \rightarrow \bar{\mathbb{R}}$ where X is a metric space and Y is a compact metric space. Define $g : X \rightarrow \bar{\mathbb{R}}$ by $g(x) = \inf_{y \in Y} f(x, y)$. Suppose for $x \in X$, the function f is jointly continuous on $V(x) \times Y$ for some neighbourhood $V(x)$ of x , then g is continuous at x .*

Proof. The upper-semicontinuity of g follows from Lemma 4. Its lower-semicontinuity follows from Lemma 13. These two results imply its continuity. \square

We are now ready to prove the following important result.

Proposition 15. *For a non-degenerate state in the canonical form, the principal radius $r[\varrho, \mu]$ is also lower-semicontinuous in μ .*

Proof. With $\varrho = (\mathbf{a}, T)$ and $C = (c_0, \mathbf{c})$, we recall the fraction function

$$F[\varrho, \mu, C] = \frac{\int d\mu(\mathbf{v}) |c_0 + \mathbf{c}^T \mathbf{v}|}{\|c_0 \mathbf{a} + T \mathbf{c}\|}, \quad (\text{P8})$$

where $C = (c_0, \mathbf{c})$ is subject to the canonical constraint $-1 \leq c_0 \leq +1$ and $\|\mathbf{c}\| = 1$.

Our purpose is to show that $F[\varrho, \mu, C]$ is jointly continuous in μ and C . In fact, the fraction function $F[\varrho, \mu, C]$ is continuous almost everywhere (including those where the denominator vanishes but the numerator is strictly positive). The only points we have to inspect are those where both the numerator and the denominator vanish. These points, however, do not exist for non-degenerate canonical states.

Indeed, the numerator vanishes, i.e., $\int d\mu(\mathbf{v}) |c_0 + \mathbf{c}^T \mathbf{v}| = 0$, implies that $c_0 + \mathbf{c}^T \mathbf{v} = 0$ is of measure 1. However the minimal requirement imposes that $\int d\mu(\mathbf{v}) \mathbf{v} = 0$. This is only possible when $c_0 = 0$. However when $c_0 = 0$, the denominator never vanishes if T is non-degenerate.

Thus we have shown that $F[\varrho, \mu, C]$ is jointly continuous in μ and C . By Corollary 14, $r[\varrho, \mu] = \inf_C F[\varrho, \mu, C]$ is also continuous in μ . (Note that we have shown the upper-semicontinuity of $r[\varrho, \mu]$ more generically in Proposition 5; here the conclusion on continuity only adds the information on its lower-semicontinuity.) \square

Remark 1. The lower-semicontinuity of the principal radius of canonical states on degenerate states perhaps also holds. The detailed analysis is however tedious. To support what follows, it is sufficient for us to restrict to non-degenerate states; but see also Section U 6.

Appendix Q: Finiteness of the critical radius

Proposition 16. *The critical radius is finite except for states of the form $\frac{\mathbb{1}}{2} \otimes \varrho_B$.*

Proof. To show that $R[\varrho]$ is finite, we will show that $r[\varrho, \mu]$ is bounded. It is obvious that $r[\varrho, \mu]$ is lower-bounded by 0. To show that $r[\varrho, \mu]$ is upper-bounded, we observe that

$$\frac{\int d\mu(\sigma) |\langle C, \sigma \rangle|}{\sqrt{2} \|\text{Tr}_B[\bar{\varrho}(\mathbb{1}_A \otimes C)]\|} \leq \frac{\int d\mu(\sigma) \|\sigma\| \|C\|}{\sqrt{2} \|\text{Tr}_B[\bar{\varrho}(\mathbb{1}_A \otimes C)]\|}, \quad (\text{Q1})$$

for any probability measure μ by Cauchy–Schwarz inequality, or

$$\frac{\int d\mu(\sigma) |\langle C, \sigma \rangle|}{\sqrt{2} \|\text{Tr}_B[\bar{\varrho}(\mathbb{1}_A \otimes C)]\|} \leq \frac{\|C\|}{\|\text{Tr}_B[\bar{\varrho}(\mathbb{1}_A \otimes C)]\|}. \quad (\text{Q2})$$

So

$$R[\varrho] = \max_{\mu} r[\varrho, \mu] \leq \inf_C \frac{\|C\|}{\|\text{Tr}_B[\bar{\varrho}(\mathbb{1}_A \otimes C)]\|}, \quad (\text{Q3})$$

where the right-hand-side is certainly upper-bounded except for $\bar{\varrho} = 0$, or $\varrho = \frac{\mathbb{1}}{2} \otimes \varrho_B$. \square

Appendix R: Continuity of the critical radius

While it is desirable to have some feeling of the continuity of the critical radius, this section is technically only needed to demonstrate the closeness of the set of unsteerable states. Readers who are more interested in the practical computation of the critical radius can thus safely skip this section.

The continuity of the critical radius is a bit subtle. In this section, we will have to consider non-degenerate states more explicitly. We will study the continuity of the critical radius when restricted to certain subsets of the defining domain of the critical radius (c. f., Section G): starting from canonical non-degenerate and general canonical states, then extending to non-degenerate normal states and normal states. Within each subset, we will use the notion of relative continuity, which is the continuity with respect to the topology of the subset. Note that when the subset under consideration is not open, this is different from the notion of continuity at every point of the subset when considering the function over the whole defining domain.

As the topology of the considered subsets matters, we note also that the set of normal states is convex and inherits a natural topology of the defining domain of the critical radius (which inherits the topology of the operator space). The set of abnormal states is closed (since the constraint is closed), and thus the set of normal states is open. The set of canonical states is convex and closed.

Proposition 17. *The critical radius function R is upper-semicontinuous relatively in the set of (degenerate and non-degenerate) canonical states.*

Proof. Because the fraction function $F[\varrho, \mu, C]$ is upper-semicontinuous jointly in (ϱ, μ) , we have that $r[\varrho, \mu]$ is jointly upper-semicontinuous in (ϱ, μ) by Lemma 4. Applying Lemma 13 (with lower-semicontinuity replaced by upper-semicontinuity and infimum replaced by supremum), we then find that $R[\varrho]$ is upper-semicontinuous. Note that the requirement that ϱ is in the canonical form is indispensable: only in this case the minimal requirement for μ is independent of ϱ and one can apply Lemma 13. \square

Proposition 18. *The critical radius function R is continuous relatively in the set of non-degenerate canonical states.*

Proof. The proof is similar to the above proof. Here we note that $F[\varrho, \mu, C]$ is continuous in all variables when ϱ is limited to non-degenerate canonical states (for the same reason as in the proof of Proposition 15). This guarantees that $r[\varrho, \mu]$ is jointly continuous in (ϱ, μ) by Corollary 14. Applying this corollary again for $r[\varrho, \mu]$, we find that $R[\varrho]$ is continuous relatively in the set of non-degenerate canonical states. \square

Proposition 19. *The critical radius is upper-semicontinuous relatively in the set of normal states and continuous relatively in the set of non-degenerate normal states.*

Proof. On (non-degenerate or general) normal states, the critical radius function can be considered as a composition of a map from (non-degenerate or general) normal states to (non-degenerate or general) canonical states, and the map from the canonical states to their critical radius values. The former map (i.e., the map from normal states to canonical states) is continuous, and the latter is continuous relatively in the set of non-degenerate canonical states or upper-semicontinuous relatively in the set of canonical states due to the above propositions. Their composition is thus also continuous or upper-semicontinuous, respectively. \square

Remark 2. It perhaps also holds that the critical radius is continuous relatively in the set of all normal states, including the degenerate ones. The analysis is again tedious.

The continuity of the critical radius breaks down at abnormal product states. It is easy to see that the critical radius is discontinuous at pure product states. Indeed, for all pure entangled states, the critical radius is $\frac{1}{2}$, but it jumps to 1 at pure product states.

Nevertheless, the upper-semicontinuity still holds at abnormal product states:

Proposition 20. *The critical radius is upper-semicontinuous at states in the union of normal states and abnormal product states.*

Note that here we can use the notion of continuity instead of relative continuity.

Proof. Note that the set of normal states is open in the defining domain of the critical radius. Upper-semicontinuity relatively in the open set of normal states implies its upper-semicontinuity at normal states when considering the function over the whole defining domain. Now we consider abnormal product states, $\varrho = (\mathbf{a}, \mathbf{a}\mathbf{b}^T, \mathbf{b})$. For any sequence $(\mathbf{a}_n, T_n, \mathbf{b}_n) \rightarrow (\mathbf{a}, \mathbf{a}\mathbf{b}^T, \mathbf{b})$ (note that states in the sequence can be normal or abnormal), we have

$$r[(\mathbf{a}_n, T_n, \mathbf{b}_n), \mu] = \inf_{c_0, \mathbf{c}} \frac{\int d\mu(\mathbf{v}) |c_0 + \mathbf{c}^T \mathbf{v}|}{\|c_0 \mathbf{a}_n + T_n \mathbf{c}\|} \leq \frac{1}{\|\mathbf{a}_n\|}. \quad (\text{R1})$$

This upper-bound is obtained by limiting the infimum to $\mathbf{c} = 0$. Therefore we also have $R[(\mathbf{a}_n, T_n, \mathbf{b}_n)] \leq \frac{1}{\|\mathbf{a}_n\|}$. So $\overline{\lim}_{n \rightarrow \infty} R[(\mathbf{a}_n, T_n, \mathbf{b}_n)] \leq \overline{\lim}_{n \rightarrow \infty} \frac{1}{\|\mathbf{a}_n\|} = \frac{1}{\|\mathbf{a}\|} = R[(\mathbf{a}, \mathbf{a}\mathbf{b}^T, \mathbf{b})]$. This implies that R is upper-semicontinuous at $\varrho = (\mathbf{a}, \mathbf{a}\mathbf{b}^T, \mathbf{b})$. \square

From the above proof, one may find that the robustness of the upper-semicontinuity of the critical radius is somewhat surprising. It in particular implies that the critical radius is upper-semicontinuous relatively in the entire set of proper states. Nevertheless, we see shortly below that this upper-semicontinuity underlies the closeness of the set of unsteerable states—something we would naturally expect. It is reasonable to expect that the upper-semicontinuity of the critical radius eventually breaks down at abnormal, non-product states. However, these pathological states are improper states and of no physical interest.

Appendix S: Levels of the critical radius

For $t \in \mathbb{R}$, we define $C_t = \{\varrho : R[\varrho] \geq t\}$. Note that here C_t contains also improper states by our convention, c. f. Section G. The intersection of C_t with the set of proper states is denoted by Q_t as in the main text. In particular, Q_1 is the set of all unsteerable proper states.

Proposition 21. *For any $t > 0$, the level set C_t is bounded.*

Proof. The boundedness of C_t is obtained by an upper-bound for R . First, we notice that in the fraction function, we can assume C is bounded. Therefore the numerator of the fraction function is bounded. Therefore

$$R[\varrho] \leq \frac{A}{\sup_{c_0, \mathbf{c}} \|c_0 \mathbf{a} + T \mathbf{c}\|}, \quad (\text{S1})$$

for some constant A .

So $R[\varrho] \geq t > 0$ implies $\sup_{c_0, \mathbf{c}} \|c_0 \mathbf{a} + T \mathbf{c}\| \leq A/t < +\infty$, which implies both \mathbf{a} and T are bounded. (Note that \mathbf{b} is always bounded within Bob's Bloch sphere.) \square

Proposition 22. *For any $t > 0$, the level set C_t is closed relatively in the union of normal states and abnormal product states.*

Proof. This is a direct consequence of the upper-semicontinuity of R over the union of normal states and non-normal product states, c. f. Proposition 20. \square

Remark 3. When considered in the whole defining domain of the critical radius (or in set of all states), the set C_t may not be closed at the (non-physical) abnormal non-product states.

Proposition 23. *For any $t > 0$, the level set C_t is convex.*

Proof. The proposition is vacuous when C_t is empty, so we assume that it is not empty. Suppose $R[\varrho_1] \geq t$ and $R[\varrho_2] \geq t$, we want to prove that for all $\lambda_1, \lambda_2 \geq 0$, $\lambda_1 + \lambda_2 = 1$ we have $R[\varrho_0] \geq t$ with $\varrho_0 = \lambda_1 \varrho_1 + \lambda_2 \varrho_2$. Let μ_1 and μ_2 be two optimal LHS ensemble for ϱ_1 and ϱ_2 , respectively. Then for $i = 1, 2$, we have $R[\varrho_i] = r[\varrho_i, \mu_i]$. From the definition, we have

$$\inf_C \frac{\int d\mu_i(\sigma) |\langle C, \sigma \rangle|}{\sqrt{2} \|\text{Tr}_B[\bar{\varrho}_i(\mathbb{1}_A \otimes C)]\|} \geq t, \quad (\text{S2})$$

with $\bar{\varrho}_i = \varrho_i - \frac{\mathbb{1}_A}{2} \otimes \varrho_B$. Since the denominator is positive, this is equivalent to

$$\int d\mu_i(\sigma) |\langle C, \sigma \rangle| \geq t\sqrt{2} \|\text{Tr}_B[\bar{\varrho}_i(\mathbb{1}_A \otimes C)]\| \quad (\text{S3})$$

for all C . Multiplying the two sides with λ_i and summing over i , we have

$$\int d\mu_0(\sigma) |\langle C, \sigma \rangle| \geq t \sum_{i=1}^2 \lambda_i \sqrt{2} \|\text{Tr}_B[\bar{\varrho}_i(\mathbb{1}_A \otimes C)]\|, \quad (\text{S4})$$

where $\mu_0 = \lambda_1 \mu_1 + \lambda_2 \mu_2$. Then using the triangular inequality, we have

$$\sum_{i=1}^2 \lambda_i \sqrt{2} \|\text{Tr}_A[\bar{\varrho}_i(\mathbb{1}_A \otimes C)]\| \geq \sqrt{2} \|\text{Tr}_B[\bar{\varrho}_0(\mathbb{1}_A \otimes C)]\|, \quad (\text{S5})$$

with $\varrho_0 = \lambda_1 \varrho_1 + \lambda_2 \varrho_2$ and $\bar{\varrho}_0 = \varrho_0 - \frac{\mathbb{1}_A}{2} \otimes \text{Tr}_B(\varrho_0)$. Therefore

$$\int d\mu_0(\sigma) |\langle C, \sigma \rangle| \geq t\sqrt{2} \|\text{Tr}_A[\bar{\varrho}_0(\mathbb{1}_A \otimes C)]\|, \quad (\text{S6})$$

or

$$r[\varrho_0, \mu_0] = \inf_C \frac{\int d\mu_0(\sigma) |\langle C, \sigma \rangle|}{\sqrt{2} \|\text{Tr}_A[\bar{\varrho}_0(\mathbb{1}_A \otimes C)]\|} \geq t. \quad (\text{S7})$$

Thus $R[\varrho_0] \geq r[\varrho_0, \mu_0] \geq t$. \square

Corollary 24. *For two states ϱ_1 and ϱ_2 , we have $\min\{R[\varrho_1], R[\varrho_2]\} \leq R[\lambda\varrho_1 + (1-\lambda)\varrho_2]$ for all $0 \leq \lambda \leq 1$.*

Proof. Let $t = \min\{R[\varrho_1], R[\varrho_2]\}$, then ϱ_1 and ϱ_2 are both in C_t . Therefore $\lambda\varrho_1 + (1-\lambda)\varrho_2$ is also in C_t due to its convexity. It follows by definition that $R[\lambda\varrho_1 + (1-\lambda)\varrho_2] \geq t = \min\{R[\varrho_1], R[\varrho_2]\}$. \square

Remark 4. If you start to wonder: we do not expect to have $\max\{R[\varrho_1], R[\varrho_2]\} \geq R[\lambda\varrho_1 + (1-\lambda)\varrho_2]$; in particular, if ρ_1 and ρ_2 are steerable, it certainly can be the case that $\lambda\varrho_1 + (1-\lambda)\varrho_2$ is unsteerable.

As a result of these properties of C_t , its intersection with the set of proper states, i.e., Q_t , is convex and compact. In particular, the set of unsteerable proper states Q_1 is convex and compact.

For the following proposition, let us define $S_t = \{\varrho : R[\varrho] = t\}$.

Proposition 25. *For any $t > 0$, $[C_t \cap \text{ext}(C_t)] \subseteq S_t \subseteq \partial C_t$. Here $\text{ext}(C_t)$ is the set of extreme points of C_t and ∂C_t is the relative boundary of C_t .*

Note that we have not shown that C_t is closed in the Bloch hyperplane of bipartite states. Therefore in principle $\text{ext}(C_t)$ may not be a subset of C_t . Yet, as we mentioned, if $\text{ext}(C_t) \setminus C_t$ is non-empty, it contains only spurious abnormal, non-product states, which are unphysical.

Proof. (i) We start with showing that $[C_t \cap \text{ext}(C_t)] \subseteq S_t$. Suppose $\varrho \in C_t$ but $\varrho \notin S_t$, we show that $\varrho \notin \text{ext}(C_t)$.

If $0 < t < R[\varrho] < +\infty$, then we let $\tilde{\varrho} = (R[\varrho]/t)\varrho + (1 - R[\varrho]/t)\frac{\mathbb{1}_A}{2} \otimes \varrho_B$. Because $R[\tilde{\varrho}] = t$, it is in C_t . On the other hand, we have $\varrho = (t/R[\varrho])\tilde{\varrho} + (1 - t/R[\varrho])\frac{\mathbb{1}_A}{2} \otimes \varrho_B$, which gives an explicit non-trivial convex decomposition of ϱ in terms of $\tilde{\varrho}$ and $\frac{\mathbb{1}_A}{2} \otimes \varrho_B$, which are both in C_t . Therefore $\varrho \notin \text{ext}(C_t)$.

Now we consider the case $R[\varrho] = +\infty$. This implies that $R[\varrho] = \frac{\mathbb{1}_A}{2} \otimes \varrho_B$. We can then make a convex decomposition $\frac{\mathbb{1}_A}{2} \otimes \varrho_B = \frac{1}{2}[(\frac{\mathbb{1}_A}{2} + \epsilon\sigma_z) \otimes \varrho_B] + \frac{1}{2}[(\frac{\mathbb{1}_A}{2} - \epsilon\sigma_z) \otimes \varrho_B]$. Each of the states in this decomposition has critical radius $1/\epsilon$ (see Section T 1), which is larger than t if ϵ is sufficiently small. Thus for sufficiently small ϵ , both states are in C_t . Therefore also in this case ϱ cannot be an extreme point of C_t .

(ii) Now we show that $S_t \subseteq \partial C_t$. Suppose $\varrho \notin \partial C_t$, that is, ϱ is in the relative interior of C_t , we show that $\varrho \notin S_t$. By Theorem 6.4 in Ref. [39], take $\frac{\mathbb{1}_A}{2} \otimes \varrho_B \in C_t$, there exists $\epsilon > 0$ such that $(1 + \epsilon)\varrho - \epsilon\frac{\mathbb{1}_A}{2} \otimes \varrho_B$ is in C_t . So $R[(1 + \epsilon)\varrho - \epsilon\frac{\mathbb{1}_A}{2} \otimes \varrho_B] = 1/(1 + \epsilon)R[\varrho] \geq t$. It then follows that $R[\varrho] \geq (1 + \epsilon)t > t$, thus $\varrho \notin S_t$. \square

Appendix T: Analytic formula of the critical radius for certain states

1. Product states

A product state is of the form $\varrho_A \otimes \varrho_B$. If ϱ_B is pure, the state is abnormal. In this case, we however have shown in Section O that its critical radius is simply $R[\varrho_A \otimes \varrho_B] = \frac{1}{\|\mathbf{a}\|}$.

When a product state $\varrho_A \otimes \varrho_B$ is normal, one can bring it to the canonical form $\varrho_A \otimes \frac{\mathbb{1}_B}{2}$. Now this state is in fact $U(2)$ invariant, where $U(2)$ acts trivially on \mathcal{H}_A and acts as conjugation on \mathcal{H}_B . Thus an optimal choice for LHS ensemble would be the uniform distribution. The lower bound (T15) below is tight. Direct computation then also gives $R[\varrho_A \otimes \varrho_B] = R[\varrho_A \otimes \frac{\mathbb{1}_B}{2}] = \frac{1}{\|\mathbf{a}\|}$. [In more details: this is nothing but the the lower bound (T15), which is tight as the uniform distribution is optimal; also note that the correlation matrix here vanishes so the infimum can be found easily.]

2. T-states

In the canonical form, if $\mathbf{a} = 0$, we have a T -state, also known as a Bell-diagonal state. The T -states form the most interesting class of normal states where an analytical formula for the critical radius has been found [21, 22]. The central simplicity of T -state is that it carries a time-reversal symmetry on both parties. As a result, the optimal LHS ensemble can be chosen to be central symmetric on the Bloch sphere [22]. Therefore, we can set $c_0 = 0$ and the critical radius becomes

$$R[(0, T)] = \max_{\mu} \inf_{\mathbf{c}} \frac{\int d\mu(\mathbf{v}) |\mathbf{c}^T \mathbf{v}|}{\|T\mathbf{c}\|}. \quad (\text{T1})$$

It can be shown that μ can be taken to be supported only on the Bloch sphere; see Section U. It was recognised by Jevtic and her collaborators [21] that, for a T -state with correlation matrix T , the LHS ensemble generated by

$$J(\mathbf{n}) = \frac{N_T}{[\mathbf{n}^T T^{-2} \mathbf{n}]^2}, \quad (\text{T2})$$

as a distribution on the Bloch sphere with

$$N_T^{-1} = \int dS(\mathbf{n}) \frac{1}{[\mathbf{n}^T T^{-2} \mathbf{n}]^2}, \quad (\text{T3})$$

has some rather special property. Namely, the boundary of the simulated states exactly resembles the so-called steering ellipsoid [21, 40]. This leads to the conjecture that the LHS ensemble is optimal for Alice to simulate steering on Bob's system, which was later proven in Ref. [22].

Translated into our current language, for the distribution (T2), the fraction function is in fact independent of \mathbf{c} ,

$$\frac{\int dS(\mathbf{n}) J(\mathbf{n}) |\mathbf{c}^T \mathbf{n}|}{\|T\mathbf{c}\|} = 2\pi N_T |\det(T)|. \quad (\text{T4})$$

It was then proven that any deviation from $J(\mathbf{n})$ leads to a decrease in the principal radius [22]. This gives rise to an analytical formula for the critical radius of T -states as

$$R[(0, T)] = 2\pi N_T |\det(T)|. \quad (\text{T5})$$

For the case where the correlation matrix T has axial symmetry, e.g., $T = \text{diag}(s, s, t)$, R can be given in a closed form,

$$R[(0, T)] = \frac{1}{|t|} \frac{1}{1 + (1 + x^2) \frac{\text{artg}(x)}{x}}, \quad (\text{T6})$$

with $x = \sqrt{s^2/t^2 - 1}$, which can take purely imaginary values when $|s/t| < 1$.

Remark 5. In Ref. [21], the integral of the form (T4) was performed using direct computation in coordinates. Here we give a coordinate-independent computation of

the integral. This is done by relaxing the dimension of the integral. Namely, we consider the integral,

$$I = \int dV(\mathbf{r}) |\mathbf{c}^T \mathbf{r}| e^{-\mathbf{r}^T T^{-2} \mathbf{r}}, \quad (\text{T7})$$

which is taken with respect to the volume measure V over the whole 3D space of \mathbf{r} . The relation to the integral (T4) can be realised by separating the integral over the radials r and the unit vector directions \mathbf{n} , $\mathbf{r} = r\mathbf{n}$, namely

$$\begin{aligned} I &= \int dS(\mathbf{n}) \int_0^\infty dr r^3 |\mathbf{c}^T \mathbf{n}| e^{-r^2 \mathbf{n}^T T^{-2} \mathbf{n}} \\ &= \int dS(\mathbf{n}) \frac{|\mathbf{c}^T \mathbf{n}|}{[\mathbf{n}^T T^{-2} \mathbf{n}]^2} \int_0^\infty dx x^3 e^{-x^2} \\ &= \frac{1}{2} \int dS(\mathbf{n}) \frac{|\mathbf{c}^T \mathbf{n}|}{[\mathbf{n}^T T^{-2} \mathbf{n}]^2}. \end{aligned} \quad (\text{T8})$$

To perform the integral (T7), we make a variable transformation $\mathbf{r} = T\tilde{\mathbf{r}}$. This gives

$$I = |\det(T)| \|T\mathbf{c}\| \int dV(\tilde{\mathbf{r}}) |\tilde{\mathbf{c}}^T \tilde{\mathbf{r}}| e^{-\tilde{\mathbf{r}}^2}, \quad (\text{T9})$$

where $\tilde{\mathbf{c}} = T\mathbf{c}/\|T\mathbf{c}\|$ is a unit vector. The latter integral can be performed directly in spherical coordinates with the z -axis along $\tilde{\mathbf{c}}$,

$$\begin{aligned} \int dV(\tilde{\mathbf{r}}) |\tilde{\mathbf{c}}^T \tilde{\mathbf{r}}| e^{-\tilde{\mathbf{r}}^2} &= \int_0^{2\pi} d\phi \int_0^\pi d\theta \sin\theta |\cos\theta| \int_0^{+\infty} dr r^3 e^{-r^2} \\ &= \pi. \end{aligned} \quad (\text{T10})$$

Thus $I = \pi |\det(T)| \|T\mathbf{c}\|$, which, by (T8) leads to

$$\int dS(\mathbf{n}) \frac{|\mathbf{c} \cdot \mathbf{n}|}{[\mathbf{n}^T T^{-2} \mathbf{n}]^2} = 2\pi |\det(T)| \|T\mathbf{c}\|. \quad (\text{T11})$$

This in turn directly leads to (T4).

3. Some analytical bounds for the critical radius

Theorem 26. *For a non-degenerate canonical state, we have*

$$2\pi N_T |\det(T)| \geq R[\varrho] \geq \frac{2\pi N_T |\det(T)|}{1 + \|T^{-1}\mathbf{a}\|}, \quad (\text{T12})$$

where $N_T^{-1} = \int dS(\mathbf{n}) [\mathbf{n}^T T^{-2} \mathbf{n}]^{-2}$.

Note that when we set $\mathbf{a} = 0$, the state becomes a T -state and the lower bound and upper bound meet at $2\pi N_T |\det(T)|$, recovering the formula for the critical radius for T -states.

Proof. The upper bound is actually obvious, since limiting the domain of infimum by setting $c_0 = 0$ always increases the infimum. We therefore only need to prove the lower bound.

To find the lower bound, we find a minimal factor λ such that $\|c_0\mathbf{a} + T\mathbf{c}\| \leq \lambda\|T\mathbf{c}\|$ for all $\|\mathbf{c}\| = 1$ and $-1 \leq c_0 \leq +1$. It is easy to show that $\lambda = 1 + \|T^{-1}\mathbf{a}\|$ should work. This can be seen as follows. To show that $\|c_0\mathbf{a} + T\mathbf{c}\| \leq \lambda\|T\mathbf{c}\|$, we show that $\{c_0\mathbf{a} + T\mathbf{c} : -1 \leq c_0 \leq +1, \|\mathbf{c}\| = 1\} \subseteq \{\lambda T\mathbf{c} : \|\mathbf{c}\| \leq 1\}$. By applying T^{-1} to both sets, the latter is equivalent to $\{c_0T^{-1}\mathbf{a} + \mathbf{c} : -1 \leq c_0 \leq +1, \|\mathbf{c}\| = 1\} \subseteq \{\lambda\mathbf{c} : \|\mathbf{c}\| \leq 1\}$. This is the case if $\lambda \geq \max\{\|c_0T^{-1}\mathbf{a} + \mathbf{c}\| : -1 \leq c_0 \leq +1, \|\mathbf{c}\| = 1\} = 1 + \|T^{-1}\mathbf{a}\|$.

We therefore see that

$$r[\varrho, \mu] = \frac{\int d\mu(\mathbf{v})|c_0 + \mathbf{c}^T\mathbf{v}|}{\|c_0\mathbf{a} + T\mathbf{c}\|} \geq \frac{\int d\mu(\mathbf{v})|c_0 + \mathbf{c}^T\mathbf{v}|}{(1 + \|T^{-1}\mathbf{a}\|)\|T\mathbf{c}\|}, \quad (\text{T13})$$

for all μ , $\|\mathbf{c}\| = 1$ and $-1 \leq c_0 \leq +1$. So, when taking the infimum over c_0 and \mathbf{c} and the maximum over μ , we obtain

$$R[\varrho] \geq \frac{2\pi N_T |\det(T)|}{1 + \|T^{-1}\mathbf{a}\|}, \quad (\text{T14})$$

where the left-hand-side is obtained using the solution of the critical radius for T -states. \square

Corollary 27. *For a state in the canonical form $\varrho = (\mathbf{a}, T)$, we have $R[(\mathbf{a}, T)] \leq R[(p\mathbf{a}, T)]$ for all $0 \leq p \leq 1$.*

In other word, depolarising Alice's state keeping the bipartite correlations intact decrease steerability.

Proof. Note that $(p\mathbf{a}, T) = p(\mathbf{a}, T) + (1-p)(0, T)$. According to Corollary 24, we have $R[(\mathbf{a}, T)] = \min\{R[(\mathbf{a}, T)], R[(0, T)]\} \leq R[(p\mathbf{a}, T)]$. \square

Despite the fact the lower bound in equation (T12) is tight for T -states, it is often far from tight when $\mathbf{a} \neq 0$. Although we can improve the lower bound, it is perhaps only of theoretical interest. For the practical purpose, the lower bound discussed below is often better.

Theorem 28. *For a state given in the canonical form,*

$$R[\varrho] \geq \frac{1}{2} \inf_{c_0, \mathbf{c}} \frac{1 + c_0^2}{\|c_0\mathbf{a} + T\mathbf{c}\|}, \quad (\text{T15})$$

subject to the constraint $-1 \leq c_0 \leq +1$ and $|\mathbf{c}| = 1$.

Proof. By using any measure that satisfies the minimal requirement as an ansatz for the LHS ensemble, we obtain a lower bound for the critical radius. If we choose the uniform distribution supported on the Bloch sphere as the ansatz, then we can evaluate the numerator $\frac{1}{4\pi} \int dS(\mathbf{n}) |c_0 + \mathbf{c}^T\mathbf{n}| = \frac{1+c_0^2}{2}$ exactly. Using this result, we obtain (T15). \square

The uniform distribution on the Bloch sphere has been used as an ansatz to prove unsteerability of two-qubit states [20, 41]. Here we used it to get a quantitative bound for the critical radius.

Appendix U: Computation of the critical radius

1. Bringing the state to the canonical form

If the state is abnormal, we can compute the critical radius directly via formula (O3). If the state is normal, the very first step is to bring it to the canonical form.

This can be done using the following procedure. Starting with a state ϱ , one obtains $\varrho_1 = \mathbb{1}_A \otimes V_B \varrho \mathbb{1}_A \otimes V_B / \text{Tr}(\mathbb{1}_A \otimes V_B \varrho \mathbb{1}_A \otimes V_B)$ with $V_B = \sqrt{\varrho_B^{-1}}$. One then derives the Bloch tensor Θ_1 for ϱ_1 ,

$$\Theta_1 = \begin{pmatrix} 1 & \mathbf{0}^T \\ \mathbf{a}_1 & T_1 \end{pmatrix}. \quad (\text{U1})$$

Now note that local unitary transformations are implemented by local rotations of the Bloch tensor. Utilising the invariance of the critical radius under local time reversals, we can also extend from the local rotations of the Bloch tensor to the general local orthogonal transformations, including the improper rotations. To this end, we find the singular value decomposition of T_1 as $T_1 = L_1 \text{diag}(\mathbf{s}) R_1$, where L_1 and R_1 are orthogonal matrices and \mathbf{s} are singular values of T_1 . We then apply local rotations L_1^T and R_1^T on Θ_1 to obtain Θ_2 ,

$$\begin{aligned} \Theta_2 &= \begin{pmatrix} 1 & \mathbf{0}^T \\ \mathbf{0} & L_1^T \end{pmatrix} \begin{pmatrix} 1 & \mathbf{0}^T \\ \mathbf{a}_1 & T_1 \end{pmatrix} \begin{pmatrix} 1 & \mathbf{0}^T \\ \mathbf{0} & R_1^T \end{pmatrix} \\ &= \begin{pmatrix} 1 & \mathbf{0}^T \\ L_1^T \mathbf{a}_1 & \text{diag}(\mathbf{s}) \end{pmatrix}. \end{aligned} \quad (\text{U2})$$

This is the Bloch tensor representation of the canonical form.

In the following, states are assumed to be non-degenerate and in the canonical form. These would include all steerable states. Although degenerate states are separable, and thus unsteerable, later we will also remark how one can compute the critical radii for degenerate states for completeness.

2. Sandwiching the Bloch sphere between two polytopes

We would like to approximate the Bloch sphere by a discrete set of points in order to carry out the computation. Note that the concepts of principal radius and critical radius apply naturally when μ is a probability measure on some arbitrary compact set \mathcal{S} , provided its convex hull contains Bob's reduced state (which is the center of the Bloch sphere, since the bipartite state is in the canonical form). The latter requirement is to make sure that the minimal requirement does not result in an empty set of measures. Indeed, for a compact subset \mathcal{S} of the Bloch hyperplane, for which the convex hull contains the center of the Bloch sphere and a probability measure μ on \mathcal{S} satisfying the minimal requirement, $\int_{\mathcal{S}} d\mu(\sigma) \sigma = \frac{\mathbb{1}_B}{2}$,

we can naturally define the fraction function

$$F^{\mathcal{S}}[\varrho, \mu, C] = \frac{\int_{\mathcal{S}} d\mu(\sigma) |\langle C, \sigma \rangle|}{\|\text{Tr}_B[\bar{\varrho} \mathbb{1}_A \otimes C]\|}, \quad (\text{U3})$$

where $\bar{\varrho} = \varrho - \frac{\mathbb{1}_A}{2} \otimes \varrho_B$. The principal radius is defined by

$$r^{\mathcal{S}}[\varrho, \mu] = \inf_C F^{\mathcal{S}}[\varrho, \mu, C]. \quad (\text{U4})$$

It is again possible to show that $r^{\mathcal{S}}[\varrho, \mu]$ is upper-semicontinuous in μ . We then define the critical radius to be

$$R^{\mathcal{S}}[\varrho] = \max_{\mu} r^{\mathcal{S}}[\varrho, \mu], \quad (\text{U5})$$

where μ are Borel measures on \mathcal{S} subjected to the minimal requirement.

The following theorem then allows us to compare the critical radius defined on nesting convex sets.

Theorem 29. *In the Bloch hyperplane, suppose a compact set \mathcal{S}_1 is contained in the convex hull of a compact set \mathcal{S}_2 , then for a non-degenerate canonical state ϱ , we have $R^{\mathcal{S}_1}[\varrho] \leq R^{\mathcal{S}_2}[\varrho]$.*

Proof. For non-degenerate canonical states, $r^{\mathcal{S}_1}[\varrho, \mu]$ is continuous in μ . This is obtained by adapting the proof of Proposition 15. Our strategy is to show that $r^{\mathcal{S}_1}[\varrho, \mu] \leq R^{\mathcal{S}_2}[\varrho]$ on the set of finitely-supported probability measures, which is dense in the set of all Borel probabilistic measures [42]. In fact we show that, for all finitely-supported measures μ on \mathcal{S}_1 satisfying the minimal requirement constraint, there exists a measure ν satisfying the minimal requirement on \mathcal{S}_2 such that $r^{\mathcal{S}_1}[\varrho, \mu] \leq r^{\mathcal{S}_2}[\varrho, \nu]$. The latter is established if we can show that $\mathcal{K}(\mu) \subseteq \mathcal{K}(\nu)$.

Indeed, suppose the measure μ on \mathcal{S}_1 is characterised by discrete weights $\{u_i\}_{i=1}^N$ at discrete 3D vectors $\{\mathbf{t}_i\}_{i=1}^N$ on the Bloch hyperplane. Because \mathbf{t}_i is in the convex hull of \mathcal{S}_2 , there exists a convex decomposition of each \mathbf{t}_i into finite M_i points $\{\mathbf{r}_j\}_{j=1}^{M_i}$ of \mathcal{S}_2 (Caratheodory's principle),

$$\mathbf{t}_i = \sum_{j=1}^{M_i} q_j^i \mathbf{r}_j^i, \quad (\text{U6})$$

where $q_j^i \geq 0$ and $\sum_{j=1}^{M_i} q_j^i = 1$. So far we ignore the zeroth coordinate of the Bloch vectors in the full operator space, which are simply 1. Taken this zeroth coordinate into account, we can write

$$\begin{pmatrix} 1 \\ \mathbf{t}_i \end{pmatrix} = \sum_{j=1}^{M_i} q_j^i \begin{pmatrix} 1 \\ \mathbf{r}_j^i \end{pmatrix}. \quad (\text{U7})$$

The set $\cup_{i=1}^N \{\mathbf{r}_j^i\}_{j=1}^{M_i}$ thus contains at most finite number of elements, and is denoted by $\{\mathbf{r}_k\}_{k=1}^M$. The convex decomposition above can be extended to run over all M

vectors, with coefficient q_k^i set to zero when not defined so that we can write

$$\begin{pmatrix} 1 \\ \mathbf{t}_i \end{pmatrix} = \sum_{k=1}^M q_k^i \begin{pmatrix} 1 \\ \mathbf{r}_k \end{pmatrix}, \quad (\text{U8})$$

with $\sum_{k=1}^M q_k^i = 1$.

Then we define the weights v_k at \mathbf{r}_k by

$$v_k = \sum_{i=1}^N q_k^i u_i. \quad (\text{U9})$$

We claim that these weights $\{v_k\}_{k=1}^M$ define a discrete measure ν on \mathcal{S}_2 that has the desired properties.

Indeed, for the minimal requirement, it is easy to see that

$$\sum_{k=1}^M v_k \mathbf{r}_k = \sum_{k=1}^M \sum_{i=1}^N q_k^i u_i \mathbf{r}_k \quad (\text{U10})$$

$$= \sum_{i=1}^N u_i \mathbf{t}_i. \quad (\text{U11})$$

To show that $\mathcal{K}(\mu) \subseteq \mathcal{K}(\nu)$, we pick up an element K of $\mathcal{K}(\mu)$ and show that $K \in \mathcal{K}(\nu)$. By the definition of $\mathcal{K}(\mu)$, there exist coefficients $\{g_i\}_{i=1}^N$, $0 \leq g_i \leq 1$, such that

$$K = \sum_{i=1}^N g_i u_i \begin{pmatrix} 1 \\ \mathbf{t}_i \end{pmatrix}. \quad (\text{U12})$$

Therefore, using (U8),

$$K = \sum_{i=1}^N \sum_{k=1}^M g_i u_i q_k^i \begin{pmatrix} 1 \\ \mathbf{r}_k \end{pmatrix} \quad (\text{U13})$$

$$= \sum_{k=1}^M \sum_{i=1}^N g_i u_i q_k^i \begin{pmatrix} 1 \\ \mathbf{r}_k \end{pmatrix} \quad (\text{U14})$$

Let us fix k . Because $0 \leq g_i \leq 1$, (due to the mean value theorem in the discrete form) there exist $0 \leq f_k \leq 1$ such that

$$\sum_{i=1}^N g_i u_i q_k^i = f_k \sum_{i=1}^N u_i q_k^i. \quad (\text{U15})$$

Thus we have

$$K = \sum_{k=1}^M f_k v_k \begin{pmatrix} 1 \\ \mathbf{r}_k \end{pmatrix}, \quad (\text{U16})$$

for $0 \leq f_k \leq 1$, or $K \in \mathcal{K}(\nu)$. \square

The following corollary is a direct consequence of the above theorem.

Corollary 30. *For a compact convex set \mathcal{S} on the Bloch hyperplane containing the center of the Bloch sphere and with compact set of extreme points $\text{ext}(\mathcal{S})$, we have $R^{\mathcal{S}}[\varrho] = R^{\text{ext}(\mathcal{S})}[\varrho]$ for a non-degenerate canonical state ϱ .*

Proof. Since \mathcal{S} is convex and compact, $\text{ext}(\mathcal{S}) \subseteq \mathcal{S}$. It follows that $R^{\mathcal{S}}[\varrho] \geq R^{\text{ext}(\mathcal{S})}[\varrho]$. On the other hand, \mathcal{S} is inside the convex hull of $\text{ext}(\mathcal{S})$, by the above theorem, we have $R^{\mathcal{S}}[\varrho] \leq R^{\text{ext}(\mathcal{S})}[\varrho]$. Therefore $R^{\mathcal{S}}[\varrho] = R^{\text{ext}(\mathcal{S})}[\varrho]$. \square

Applied to the Bob's Bloch ball, this corollary implies that the LHS ensemble in equation (4) in the main text can be assumed to be supported on the Bloch sphere (i. e., the pure states), excluding the mixed states. This fact has been actually often assumed in the literature without a proper proof.

Computationally, the above theorem allows us to lower-bound and upper-bound the critical radius of a non-degenerate canonical state by approximating the Bloch sphere by a finite number of points. To be specific, let \mathcal{S}_B^- and \mathcal{S}_B^+ be the sets of vertices of two convex polytopes such that $\text{conv} \mathcal{S}_B^- \subseteq \mathcal{B}_B \subseteq \text{conv} \mathcal{S}_B^+$. When the polytopes are fixed by context, we denote $R^+[\varrho] = R^{\mathcal{S}_B^+}[\varrho]$ and $R^-[\varrho] = R^{\mathcal{S}_B^-}[\varrho]$ for simplicity. We then have $R^-[\varrho] \leq R[\varrho] \leq R^+[\varrho]$. In practice, we can choose \mathcal{S}_B^- on Bob's Bloch sphere \mathcal{S}_B itself, and \mathcal{S}_B^+ such that the surface of its convex hull circumscribes \mathcal{S}_B . With sufficient high numbers of vertices where both \mathcal{S}_B^- and \mathcal{S}_B^+ are good approximations for \mathcal{S}_B , we can expect to have a good approximation for $R[\varrho]$. This is indeed the case due to the bound of errors discussed below.

A note on convention: in the following, polytopes are always assumed to be convex. Here and in the following a polytope may mean the set of its vertices or the whole convex polytope itself. This ambiguity should not cause any confusion, since it should be clear from the context what is meant by a polytope.

3. Universal bound of the relative error

In practice, it is convenient to choose \mathcal{S}_B^- as a discrete set on the Bloch sphere *with the inversion symmetry*. Let r_{in} be the inscribed radius of the polytope \mathcal{S}_B^- . Note that due to the inversion symmetry, the center of the inscribed sphere of the polytope is at the origin. We then define the enlarged polytope $\mathcal{S}_B^+ = \{\mathbf{v} = \eta \mathbf{n} : \mathbf{n} \in \mathcal{S}_B^-\}$ with $\eta = 1/r_{\text{in}}$. The enlarged polytope then contains the Bloch ball. We therefore have that $R^-[\varrho] \leq R[\varrho] \leq R^+[\varrho]$. More interestingly, we also have $R^+[\varrho] \leq \eta R^-[\varrho]$, which leads to a universal bound of the relative error to be $1/\eta - 1$, regardless of the details of the input state.

Theorem 31. *Consider a polytope \mathcal{S}_B^- with inversion symmetry and $\mathcal{S}_B^+ = \{\mathbf{v} = \eta \mathbf{n} : \mathbf{n} \in \mathcal{S}_B^-\}$ with $\eta = 1/r_{\text{in}}$. For a canonical state ϱ , we have $R^+[\varrho] \leq \eta R^-[\varrho]$.*

Proof. For simplicity, we denote the canonical state ϱ by (\mathbf{a}, T) and as before, we write $R^\pm[\varrho] = R^\pm[(\mathbf{a}, T)]$. Then we have $R^+[(\mathbf{a}, T)] = \eta R^-[(\eta \mathbf{a}, T)]$. To see this, we start

$$\begin{aligned} R^+[(\mathbf{a}, T)] &= \max_{\mu} \inf_{c_0, \mathbf{c}} \frac{\int_{\mathcal{S}_B^+} d\mu(\mathbf{v}) |c_0 + \mathbf{c}^T \mathbf{v}|}{\|c_0 \mathbf{a} + T \mathbf{c}\|} \\ &= \max_{\mu} \inf_{c_0, \mathbf{c}} \frac{\int_{\mathcal{S}_B^-} d\mu(\mathbf{n}) |c_0 + \eta \mathbf{c}^T \mathbf{n}|}{\|c_0 \mathbf{a} + T \mathbf{c}\|} \\ &= \max_{\mu} \inf_{c_0, \mathbf{c}} \frac{\int_{\mathcal{S}_B^-} d\mu(\mathbf{n}) |\eta c_0 + \eta \mathbf{c}^T \mathbf{n}|}{\|\eta c_0 \mathbf{a} + T \mathbf{c}\|} \\ &= \eta \max_{\mu} \inf_{c_0, \mathbf{c}} \frac{\int_{\mathcal{S}_B^-} d\mu(\mathbf{n}) |c_0 + \mathbf{c}^T \mathbf{n}|}{\|\eta c_0 \mathbf{a} + T \mathbf{c}\|} \\ &= \eta R^-[(\eta \mathbf{a}, T)]. \end{aligned} \quad (\text{U17})$$

In the above manipulation, note that μ is just a discrete measure defined by a finite probability weights on \mathcal{S}_B^- or \mathcal{S}_B^+ (the integral thus can be replaced by a discrete sum).

We now only need to show that for $\eta \geq 1$, $R^-[(\eta \mathbf{a}, T)] \leq R^-[(\mathbf{a}, T)]$. This is in fact the content of Corollary 27, except that there \mathcal{S}_B^- is replaced by the whole Bloch ball \mathcal{B}_B . We thus just need to investigate the validity of the corollary when the Bloch sphere is approximated by \mathcal{S}_B^- . Corollary 27 is in turn based on Corollary 24, thus Proposition 23 and the upper bound in Theorem 26. We now inspect their validity.

(i) Proposition 23 in fact makes no use of any property of the Bloch sphere and works just fine for \mathcal{S}_B^- . The level set $C_t^- = \{(\mathbf{a}, T) : R^{\mathcal{S}_B^-}[(\mathbf{a}, T)] \geq t\}$ is thus indeed convex. Corollary 24 is also valid.

(ii) The upper bound in Theorem 26 is obtained by restricting the domain of infimum to $c_0 = 0$. We then need to show that

$$R^{\mathcal{S}_B^-}[(0, T)] = \inf_{\mathbf{c}} \frac{\int_{\mathcal{S}_B^-} d\mu(\mathbf{v}) |\mathbf{c}^T \mathbf{v}|}{\|T \mathbf{c}\|}. \quad (\text{U18})$$

The latter means that c_0 can indeed be set to 0 in the definition of $R^{\mathcal{S}_B^-}[(0, T)]$ for T -states. This is based on the fact that T -states $(0, T)$ have the time-reversal symmetry implemented by the inversion of the operator space, which implies that the LHS ensemble μ can be chosen to be central symmetric. One then simply notes that this whole procedure remains valid for the approximated Bloch sphere \mathcal{S}_B^- provided \mathcal{S}_B^- has the inversion symmetry. \square

While one somehow might have anticipated the bound $R^+[\varrho] \leq R^-[\varrho]/r_{\text{in}}$, in the above proof, the inversion symmetry of the polytope (which is nothing but time-reversal symmetry) enters in a rather subtle way. We see once again the fundamental role of time-reversal symmetry in quantum steering, which seemed to be overlooked.

4. Optimise the principal radius over probability distributions on a polytope

It is now left to describe an algorithm to compute $R^{\mathcal{S}}[\varrho]$ where \mathcal{S} is the set of vertices of a polytope. As μ is finitely supported on \mathcal{S} , $\mathcal{K}(\mu)$ is in fact a polytope of finite vertices and faces. In this case, the minimisation to compute the principal radius (E1) can be limited to operators C which are normal vectors of the proper faces of maximal dimension of $\mathcal{K}(\mu)$. In that way, to compute the critical radius (E1) we only need to solve a linear program of finite size.

In Ref. [20], the characterisation of vertices of such a polytope $\mathcal{K}(\mu)$ in the 4D space is worked out in details. The technique boils down to take a direction, dictated by an operator C and find the maximisers $\arg \max_{K \in \mathcal{K}(\mu)} \langle C, K \rangle$, which is simply a linear maximisation. It was shown that the maximisers are of the form

$$K^* = \int_{\mathcal{S}} d\mu(\sigma) [\chi_{\langle C, \sigma \rangle > 0}(\sigma) + \chi_{\langle C, \sigma \rangle = 0}(\sigma) g(\sigma)] \sigma, \quad (\text{U19})$$

where $\chi_X(\sigma)$ is the characteristic function of the set X and $g(\sigma)$ is an arbitrary function with values between 0 and 1. This has a simple interpretation: the maximisers are the sum of all members of the local hidden states which have positive projections on C indicated by $\chi_{\langle C, \sigma \rangle > 0}$, and members that are orthogonal to C indicated by $\chi_{\langle C, \sigma \rangle = 0}$ does not change the maximum. The maximal value is

$$\langle C, K^* \rangle = \int_{\mathcal{S}} d\mu(\sigma) \max\{\langle C, \sigma \rangle, 0\}, \quad (\text{U20})$$

independent of $g(\sigma)$. This independence of the maximal value upon $g(\sigma)$ in the maximiser (U19) tells that the maximisation problem $\max_{K \in \mathcal{K}(\mu)} \langle C, K \rangle$ may have multiple maximisers, characterised by $g(\sigma)$. These maximisers form faces of $\mathcal{K}(\mu)$. Certainly, if the plane $\langle C, \sigma \rangle = 0$ does not go through any vertex of $\mathcal{K}(\mu)$, $g(\sigma)$ does not contribute to the maximiser (U19) and the maximiser is unique. On the other hand, if the plane $\langle C, \sigma \rangle = 0$ goes through a vertex, the function $g(\sigma)$ can be adjusted such that this point is included in the whole integral (U19) or not, giving $2^1 = 2$ independent extreme points of $\mathcal{K}(\mu)$, which form a line segment of maximisers. We are interested in the case where the plane $\langle C, \sigma \rangle = 0$ goes through (at least) 3 points, where (U19) gives $2^3 = 8$ different extreme points of $\mathcal{K}(\mu)$ forming a proper face of $\mathcal{K}(\mu)$ with maximal dimension (i.e., of dimension 3). This argument leads to a correspondence between planes that go through 3 points of \mathcal{S} and proper faces of maximal dimension of $\mathcal{K}(\mu)$. The correspondence actually goes much further: suppose c_0 and \mathbf{c} are the offset and the normal vector of a plane that goes through 3 points of \mathcal{S} , then (c_0, \mathbf{c}) is the 4D normal vector of a maximal face of $\mathcal{K}(\mu)$. Crucially, one also finds that the set of 4D normal vectors of the maximal faces of $\mathcal{K}(\mu)$ depends only on the chosen polytope, and not on the probability measure μ .

If \mathcal{S} consists of N vertices, then the linear program (U5) has N variables (apart from some slack variables). There are $N(N-1)(N-2)/6$ planes that go through three points in \mathcal{S} . Together with the constraints on the positivity of the probability weights, we have $N(N-1)(N-2)/6 + N$ inequality constraints. In addition, the minimum requirement gives 4 equality constraints. Over all, we have a linear program of $\mathcal{O}(N)$ variables and $\mathcal{O}(N^3)$ constraints.

5. Implication of the symmetry of the state

When the state has some symmetry, we can exploit the symmetry to simplify the optimisation as well. Theorem 7 implies that if a state ϱ has symmetry group \mathcal{G} , then one can assume that the optimal LHS ensemble μ is symmetric under \mathcal{G} . When the Bloch sphere is approximated by a polytope \mathcal{S} , not only the symmetry of the state ϱ matters, but also does the symmetry of \mathcal{S} . We have the restricted symmetry theorem.

Proposition 32 (Restricted symmetry of LHS ensemble). *If for a compact group \mathcal{G} , ϱ is (\mathcal{G}, U, V) symmetric, the polytope \mathcal{S} is (\mathcal{G}, V) symmetric, then there exists an optimal ensemble μ^* on \mathcal{S} which is (\mathcal{G}, V) -invariant, $R_V(g)[\mu^*] = \mu^*$.*

Proof. The proof is actually rather the same as that of Theorem 7. Here the fact that \mathcal{S} is symmetric under \mathcal{G} just ensures the consistency of the proof: the space of probability measures on \mathcal{S} is also symmetric under \mathcal{G} . \square

6. Remark on the computation for degenerate states

Note that even if the (canonical) states are close to degenerate, our procedure is still valid. Truly degenerate canonical states are not of the main interest, we nevertheless sketch how to cope with them for completeness.

For truly degenerate state, strictly Proposition 15 on the continuity of the principal radius in principle may not apply, and thus neither does Theorem 29. We are back at the tedious problem of demonstrating the continuity of the principal radius with respect to LHS ensemble μ for degenerate states. For the practical purpose, there is a work around, though. The idea is that for degenerate states, both μ and C can be subjected to some restrictive constraints. Under these restrictive constraints, Proposition 15 and Theorem 29 regain their validity.

Suppose T is degenerate and consider the faction function (E2),

$$F[\varrho, \mu, C] = \frac{\int d\mu(\mathbf{v}) |c_0 + \mathbf{c}^T \mathbf{v}|}{\|c_0 \mathbf{a} + T \mathbf{c}\|}. \quad (\text{U21})$$

To be concrete, we can assume $T = \text{diag}(s_1, s_2, 0)$ without loss of generality. Note that now the state is invariant

under the time-reversal transformation implemented by the reflection along z on Bob's space (by the way, this implies that they are separable). Therefore the LHS ensemble can be assumed to be symmetric under reflection along z . Further, \mathbf{c} can then be limited to be orthogonal to the kernel of T , i.e., in the xy -plane. One can easily verify that Proposition 15 is again valid if μ is limited to those that are symmetric under z -reflection and \mathbf{c} is on the xy -plane. As a result, Theorem 29 applies and the numerical procedure is valid. In fact, one can go on to show that μ can be assumed to be supported on the xy -plane, which largely simplifies the practical computation. Thus, while degenerate states seem theoretically complicated, practically they are in fact easier to work with. The case where T is rank-1 can be worked out similarly.

7. Technical aspects and the EPR-package

On the technical side, for a generic state, the vertices of the polytopes used to approximate the Bloch sphere were chosen to be the solutions of the so-called ‘‘covering problem’’ taken from Ref. [45]. These arrangements of points \mathbf{t}_i on the unit sphere have icosahedral symmetry and are arranged such that $\max_i \min_{j \neq i} \|\mathbf{t}_i - \mathbf{t}_j\|$ is minimal. This gives directly an inner polytope. For the outer polytope, we used a rescaled version of the inner polytope by the inverse of its inscribed radius. The corresponding upper bound on $R(\varrho_{AB})$ was calculated independently, i.e., without using the estimate $R_{\text{in}} \leq R(\varrho_{AB}) \leq R_{\text{in}}/r_{\text{in}}$, as this gives typically a better bound.

The linear system of equations with constraints derived from the minimal requirement, the probability bounds, and the target function in equation (E1) were written to a file in a linear program format which was then read and solved employing IBM ILOG CPLEX Optimization Studio. With a 92-vertex polytope, the computational time for a generic state is about 30 seconds on average when running on an Intel Xeon X5650 (2.67GHz) processor with six physical cores. The inscribed radius of the 92-vertex polytope is $r_{\text{in}} \approx 0.972$, thus the relative error is at most 2.8%. When highly accurate values of the critical radius are desired, one can use a 252-vertex polytope with $r_{\text{in}} \approx 0.990$, which requires about 40 minutes computation and about 48GB memory.

If the states have axial symmetry, assumed to be in z -axis, the best choice for the inner polytope is to impose some subgroup of the rotation group around a fixed axis. To this end, one can choose polytopes with vertices formed by intersecting p circles of latitude with $q = 2p + 2$ uniformly distributed great circles that go through the north and south poles. The circles of latitude can be arranged in various schemes: (i) the polar angles are uniformly distributed, (ii) the intersections with the symmetry axis are uniformly distributed, (iii) the intersections with the symmetry axis are identical to the Gauss-Legendre abscissae order p . We found that when

p and q are fixed, the last scheme gives the largest value for the inscribed radius r_{in} . Thus, we chose this scheme in our calculations.

In this case, the polytope has the axial rotation group of degree q . By Theorem 32 on the restricted symmetry of the optimal LHS ensemble, we can assume that the LHS ensembles are the same for points with the same latitude. This reduces the number of variables in the linear program by a factor of q . Moreover, many directions normal to polytope facets transform to each other under the axial rotation group of degree q . Thus the number of constraints also decreases by certain factor of order q . Consequently, the size of the linear program in computing R decreases significantly and the upper bound and lower bound for R can be obtained using polytopes with much higher number of vertices. In our computation, we were able to use $q = 52$ and $p = 25$ which results in a polytope with 1032 vertices and $r_{\text{in}} \approx 0.996$.

Our programs and examples are available at <https://gitlab.com/cn611340/epr-steering>.

Appendix V: Gradients of the critical radius

It is generally tedious to show that the critical radius is differentiable. However, at certain points such as T -states, it is plausible that the critical radius function is reasonably smooth. At these points, we can assume that the gradient exists. Gradients of the critical radius are normal vectors of the supporting hyperplanes of its level sets. They are therefore directly related to optimal steering inequalities.

We recall that any normal state can be brought to the canonical form (O4) by the group action of $U(2) \times GL(2)$. The action also allows one to relate the supporting hyperplane at a normal state with that at its canonical form and vice versa. Excluding abnormal states, we can therefore restrict ourselves to computing the gradients of the critical radius at canonical states.

Take a state $\varrho = (\mathbf{a}, \text{diag } \mathbf{s})$ in the canonical form, and let us assume that the gradient exists. Again, because of the invariance of R with respect to the action of $U(2) \times GL(2)$, we know that the gradient $\nabla R[\varrho]$ has to be orthogonal to all the flowing directions of the action of $U(2) \times GL(2)$. More precisely, we have the following lemma.

Lemma 33. *For any state ϱ , we have*

(i) *For any traceless hermitian operator H ,*

$$\langle \nabla R[\varrho], [H \otimes \mathbb{1}_B, \varrho] \rangle = 0. \quad (\text{V1})$$

(ii) *For any (complex) operator M , if we denote $K = (\mathbb{1}_A \otimes M)\varrho - \varrho(\mathbb{1}_A \otimes M^\dagger) - \varrho \text{Tr}(M \varrho_B - \varrho_B M^\dagger)$, then*

$$\langle \nabla R[\varrho], K \rangle = 0. \quad (\text{V2})$$

Proof. The equalities are obtained by considering the infinitesimal action (i.e., the Lie algebra action) associated to the action of $U(2) \times GL(2)$.

(i) Recall that the Lie algebra of $U(2)$ are traceless, skewed hermitian operators $\mathfrak{su}(2)$. For any traceless hermitian operator $H \in \mathfrak{su}(2)$, $U(t) = e^{-itH}$ with t in some neighbourhood of 0 is an element of $U(2)$ near the identity. Since R is invariant under $U(2)$, we have $\frac{d}{dt}R[U(t) \otimes \mathbb{1}_B \varrho U^\dagger(t) \otimes \mathbb{1}_B] = 0$. Computing the derivative explicitly results in (V1).

(ii) Similarly, for any operator $M \in \mathfrak{gl}(2, \mathbb{C})$, which consists of all complex matrices, we have $V(t) = e^{-itM}$ is an element of $GL(2)$ near the identity. Since R is invariant under $GL(2)$, we have $\frac{d}{dt}R[\mathbb{1}_A \otimes V(t) \varrho \mathbb{1}_A \otimes V^\dagger(t) / \text{Tr}(V(t) \varrho_B V^\dagger(t))] = 0$. Computing the derivative explicitly results in (V2). \square

Now suppose we can compute the derivatives of R with respect to the canonical parameters \mathbf{a} and \mathbf{s} , or equivalently, we know $\langle \nabla R[\varrho], \sigma_i^A \otimes \mathbb{1}_B \rangle$ and $\langle \nabla R[\varrho], \sigma_i^A \otimes \sigma_i^B \rangle$ for $i = 1, 2, 3$. We then should be able to incorporate the invariant directions in Lemma 33 to find $\nabla R[\varrho]$ explicitly. For T -states, all these can be computed explicitly.

Lemma 34. *For a non-degenerate T -state $(0, T)$ with $T = \text{diag}(\mathbf{s})$, we have:*

$$\langle \nabla R[(0, T)], \sigma_i^A \otimes \mathbb{1}_B \rangle = 0, \quad (\text{V3})$$

$$\langle \nabla R[(0, T)], \sigma_i^A \otimes \sigma_i^B \rangle = F_i(\mathbf{s}), \quad (\text{V4})$$

for $i = 1, 2, 3$, where

$$F_i(\mathbf{s}) = 2\pi \frac{\partial(|s_1 s_2 s_3| N_T)}{\partial s_i}, \quad (\text{V5})$$

with N_T defined in equation (T3).

Proof. (i) The first identity expresses the fact that at T -states, the derivative of the critical radius with respect to Alice's reduced state vanishes. Indeed, we know that for states in the canonical form $\varrho = (\mathbf{a}, T)$, due to the time-reversal symmetry, we have $R[(\mathbf{a}, T)] = R[(-\mathbf{a}, T)]$. Thus the derivative of R with respect to \mathbf{a} must vanish at $\mathbf{a} = 0$.

(ii) The second identity is obtained by directly differentiating the critical radius of T states in equation (T5) with respect to \mathbf{s} . \square

Let us reconstruct the gradient at the T -states explicitly. One can compute the invariance directions dictated by Lemma 33 directly. This computation is further simplified by noting that $\rho_B = \frac{\mathbb{1}_B}{2}$ for T -states. To find out these directions, in equation (V1), we choose $H = \sigma_k^A$ with $k = 1, 2, 3$ and in equation (V2), we choose $M = \sigma_k^B$ and $M = i\sigma_k^B$ with $k = 1, 2, 3$. This gives us 9 directions in which the gradient vanishes. Further more, when incorporating the fact that $\langle \nabla R[(\mathbf{a}, T)], \sigma_i^A \otimes \mathbb{1}_B \rangle = 0$ for all i , equation (V3), we come to the conclusion that

$\nabla R[(\mathbf{a}, T)]$ vanishes in all directions $\sigma_i^A \otimes \sigma_j^B$ for $i \neq j$. Therefore we have, for T -states,

$$\nabla R[(0, T)] = \frac{1}{16} \sum_{i=1}^3 F_i(\mathbf{s}) \sigma_i^A \otimes \sigma_i^B. \quad (\text{V6})$$

Here the prefactor $\frac{1}{16}$ is due to the normalisation for the vectors $\sigma_i^A \otimes \sigma_i^B$. Note that the expression is symmetric in two parties, as a result, the gradients for the critical radius of steering from A to B and from B to A share the same gradients at T -states. This is rather surprising given the asymmetry in the definition of quantum steering with respect to the two parties. This surprising fact is again deeply rooted in the hidden symmetry of the critical radius under time-reversal transformation, which results in the first condition in (V3).

Under the light of the relationship between gradients and supporting hyperplanes of level sets, these gradients of the critical radius certainly result in optimal steering inequalities. Despite the fact that we can actually compute the critical radius R and gives various bounds for it, these steering inequalities may still be useful for proving steerability in experiments when the full tomography of the state is not available.

Appendix W: Details of the examples

1. Random cross-sections

To construct a 2D random cross-section, we choose two random states and construct the 2D plane that goes through the maximally mixed state, $\frac{\mathbb{1}_A}{2} \otimes \frac{\mathbb{1}_B}{2}$, and these two random states. The boundary of the set of unsteerable states was obtained by solving the equation $R[\varrho] = 1$ along 200 rays going through $\frac{\mathbb{1}_A}{2} \otimes \frac{\mathbb{1}_B}{2}$. The equation was solved numerically employing the standard bisection method. The polytopes that are used to approximate the Bloch sphere and the detailed implementation are described in Section U 7.

To illustrate the results of our calculations, we selected, in an arbitrary manner, three examples of 2D random cross-sections as presented in Figure 7 where the steerability of states in the narrow gray regions is uncertain due to the numerical accuracy. Here the computation was performed using the 162-vertex polytope and the sets of unsteerable states are extended beyond proper states. The first two examples in this figure have been presented in Figure 5 of the main text, where the 252-vertex polytope was used, and only proper states were considered.

2. Symmetric cross-sections

To illustrate the symmetry of the critical radius under the local time-reversal transformations, we choose a cross-section cut by a 2D plane which is invariant under

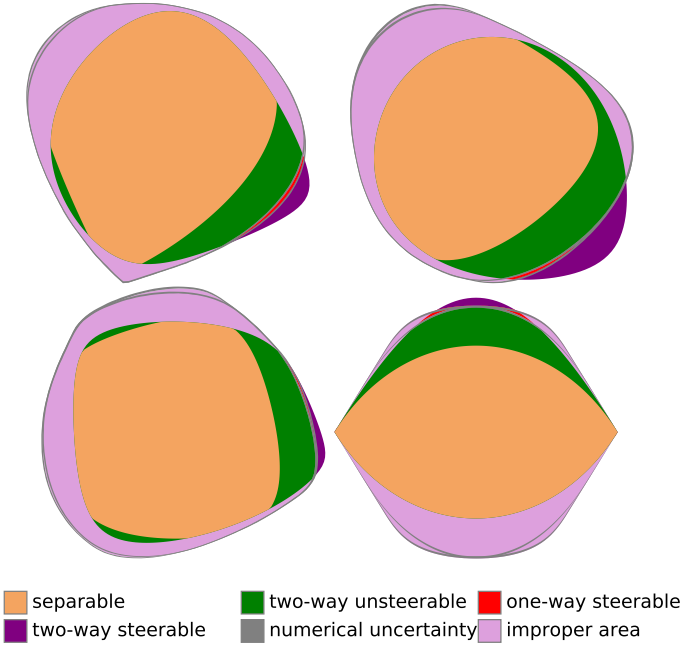


FIG. 7. Top row and lower left: random 2D cross-sections of the set of two-way steerable states, one-way steerable states, two-way unsteerable states, and separable states. Differently from the main text, here the set of states with $R[\varrho] \leq 1$ is extended beyond the set of proper states (to include improper states). Lower right: a 2D symmetric cross-sections showing the set of unsteerable states, including improper ones, that is symmetric under the time-reversal transformations implemented by the reflections and inversions as described in the text.

the local time-reversal transformations. Such a symmetric cross-section is illustrated with states in the canonical form for steering from A to B . Two random states are chosen to be $(\mathbf{a}, 0)$ and $(0, \text{diag}(\mathbf{s}))$. All states in the cross-section are of the form $x(\mathbf{a}, 0) + y(0, \text{diag}(\mathbf{s})) = (x\mathbf{a}, y \text{diag}(\mathbf{s}))$. On this plane, the time-reversal transformation on Alice's side (upto local unitary transformations) is implemented by inversion of (x, y) , while the time-reversal transformation on Bob's side is implemented by inversion of y .

Note that this cross-section contains the whole scaling lines, namely, $R[(\mathbf{a}, \mathbf{s})] = \lambda R[(\lambda\mathbf{a}, \lambda\mathbf{s})]$. This scaling relation of the critical radius provides a powerful tool for determining the boundary of the set of unsteerable states. One no longer needs to solve equation $R[\varrho] = 1$ by the bisection method. Instead, one simply computes the upper bound and lower bound for $R[(\mathbf{a}, \mathbf{s})]$ on a closed loop—here chosen to be the unit circle—and then uses the scaling relation to locate the boundary of the set of unsteerable states.

For steering from B to A , we note that the special structure of the canonical form for steering from A to B allows for a slightly different scaling relation for steering from B to A , namely $R^{B \rightarrow A}[(\mathbf{a}, \text{diag}(\mathbf{s}))] =$

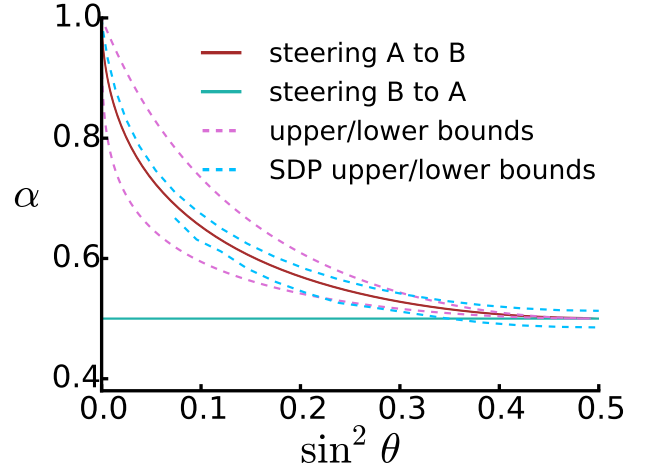


FIG. 8. Boundary of the set of one-way steerable states for the family of states described in equation (W1). The thickness of the line presenting the boundary between steerable/unsteerable states from A to B indicates the uncertainty due to numerical accuracy. The analytical upper bound is obtained using equation (T12). The analytical lower bound is obtained using equation (T15), which gives the same lower bound as Figure 3 in Ref. [41]. The SDP data are provided by the authors of Ref. [28].

$\lambda R^{B \rightarrow A}[(\mathbf{a}, \lambda \text{diag}(\mathbf{s}))]$ with $R^{B \rightarrow A}[\varrho]$ being the critical radius for steering from B to A . This scaling can also be employed to locate the boundary of unsteerable states starting from the values of R on a closed loop as for the case of steering A to B . Here the loop was chosen to be the boundary of the set of separable states. The upper bound and lower bound for $R^{B \rightarrow A}$ of states on this boundary were determined by bringing the states to its canonical form for steering from B to A and applying the same computation procedure as for steering from A to B . An example of symmetric 2D cross-sections is also shown in the bottom-right panel of Figure 7.

3. A family of one-way unsteerable states

In this section we consider the state

$$\varrho = \alpha|\theta\rangle\langle\theta| + (1 - \alpha)\varrho_A \otimes \frac{\mathbb{1}_B}{2}, \quad (\text{W1})$$

where $|\theta\rangle = \cos \frac{\theta}{2} |00\rangle + \sin \frac{\theta}{2} |11\rangle$ with $0 \leq \theta \leq \frac{\pi}{4}$ and $0 \leq \alpha \leq 1$. This state is important for demonstrating the one-way steering phenomenon [41]. As $|\theta\rangle$ is pure, it is easy to show via the scaling relation (L1) that the state is steerable from B to A for $\alpha > \frac{1}{2}$ and $\theta > 0$. However, determining the boundary of unsteerable states from A to B has been proven to be difficult [28]. Here we show how this boundary can be obtained with high accuracy in our approach.

For states of the form (W1), the boundary for unsteerable states is also obtained by solving the equation $R[\varrho] = 1$ numerically using the bisection method, similar

to the case of random cross-sections. Note that in this case the state is axially symmetric around the z -axis. We therefore can use the symmetry to reduce the size of the linear program and conveniently work with polytopes of 1032 vertices; see Section U 7.

In Figure 8, we present the obtained border between unsteerable/steerable states together with certain analytical bounds and the known data from SDP [28] for states of the form (W1). One observes that with $q = 52$ and $p = 25$, we can obtain rather accurate description of the border. Note that the regime of one-way unsteerable states looks significantly exaggerated in comparison to Figure 7; however here the parametrisation does not faithfully represent the Hilbert–Schmidt metric of the state space.

Appendix X: Generalisation to higher dimensional systems

In this section, we assume that Alice and Bob share a state ϱ of dimension $d_A \times d_B$. An n -POVM implemented by Alice is $E = \bigoplus_{i=1}^n E_i$, where $0 \leq E_i \leq \mathbb{1}_A$, $\sum_{i=1}^n E_i = \mathbb{1}_A$. Following Ref. [27], a bipartite state ϱ is unsteerable (from A to B) with respect to n -POVMs if and only if there exists a LHS ensemble μ such that

$$\int d\mu(\sigma) \max_i \{\langle Z_i, \sigma \rangle\} \geq \sum_{i=1}^n \text{Tr}[\varrho(E_i \otimes Z_i)], \quad (\text{X1})$$

for all $Z = \bigoplus_{i=1}^n Z_i$ and all POVMs $E = \bigoplus_{i=1}^n E_i$. This inequality has a simple interpretation. Upon making a measurement E on her side, Alice decomposes Bob's state into n conditional states. Bob then makes n different measurements to determine the expectation values of n arbitrary observables Z_i , each for a conditional state, and then average them out over all conditional states. If the conditional states are simulated from an LHS ensemble μ , this average clearly cannot exceed the left hand side of (X1), where each of the state in the LHS ensemble is associated to the operator Z_i that has the maximal mean value.

We then define the *inverse* fraction function $F^{-1}[\varrho, \mu, Z, E]$ to be

$$\frac{\sum_{i=1}^n \text{Tr}[\varrho(E_i \otimes Z_i)] - \frac{1}{d_A} \sum_{i=1}^n \text{Tr}(E_i) \text{Tr}(\varrho_B Z_i)}{\int d\mu(\sigma) \max_i \{\langle Z_i, \sigma \rangle\} - \frac{1}{d_A} \sum_{i=1}^n \text{Tr}(E_i) \text{Tr}(\varrho_B Z_i)}, \quad (\text{X2})$$

with the *numerator-dominated convention*, meaning, if the numerator vanishes, the function vanishes regardless of the denominator. The reason we define the inverse of the fraction function, instead of the function itself, is because the numerator of the inverse fraction function can be negative, while the denominator is non-negative. That the denominator is non-negative ensures that inequality (X1) holds if and only if $F^{-1}[\varrho, \mu, Z, E] \leq 1$. Moreover, the offset subtracted from both the numerator

and the denominator was chosen to enforce the scaling of the critical radius; see Section X 2 a below.

The inverse principal radius $r_n^{-1}[\varrho, \mu]$ is defined as

$$r_n^{-1}[\varrho, \mu] = \sup_{Z, E} F^{-1}[\varrho, \mu, Z, E]. \quad (\text{X3})$$

In difference from PVMs, the fraction function for POVMs can be negative. Yet, one can easily show that $r_n^{-1}[\varrho, \mu] \geq 0$. Then one can also write

$$r_n^{-1}[\varrho, \mu] = \sup_{Z, E} \max\{F^{-1}[\varrho, \mu, Z, E], 0\}. \quad (\text{X4})$$

Similar to Lemma 2, we can easily show that the inverse critical radius $r_n^{-1}[\varrho, \mu]$ is convex in μ , since so is $\max\{F^{-1}[\varrho, \mu, Z, E], 0\}$. Also, similar to Lemma 5, for a fixed ϱ , $r_n^{-1}[\varrho, \mu]$ is weakly lower-semicontinuous with respect to μ . Therefore $r_n^{-1}[\varrho, \mu]$ attains the minimum value for some μ^* (an optimal LHS ensemble). We define the inverse *critical radius* to be

$$R_n^{-1}[\varrho] = \min_{\mu} r_n^{-1}[\varrho, \mu], \quad (\text{X5})$$

where μ is subject to *minimal requirement*,

$$\int d\mu(\sigma) \sigma = \varrho_B. \quad (\text{X6})$$

Then the state ϱ is unsteerable if and only if $R_n[\varrho] \geq 1$.

1. Reducing to the formula for two-qubit states

We first note that both the numerator and the denominator are invariant under transformation $Z_i \rightarrow Z_i - Y$ for arbitrary hermitian operator Y . Thus we can assume $\sum_{i=1}^n Z_i = 0$. When restricted to 2-POVMs, we can set $C = Z_1 = -Z_2$. Further, for two-qubit systems, we can restrict from 2-POVMs to PVMs, thus $E_1 = Q$ with $E_2 = \mathbb{1}_A - Q$ for some projection Q . We then have

$$r_2^{-1}[\varrho, \mu] = \sup_C \frac{2 \max_Q \text{Tr}[(\varrho - \frac{\mathbb{1}_A}{2} \otimes \varrho_B)(Q \otimes C)]}{\int \mu(\sigma) |\langle C, \sigma \rangle|}. \quad (\text{X7})$$

Now note that $\text{Tr}[(\varrho - \frac{\mathbb{1}_A}{2} \otimes \varrho_B)(Q \otimes C)] = \text{Tr}\{\text{Tr}_B[(\varrho - \frac{\mathbb{1}_A}{2} \otimes \varrho_B)(\mathbb{1}_A \otimes C)]Q\}$. Since $\text{Tr}_B[(\varrho - \frac{\mathbb{1}_A}{2} \otimes \varrho_B)(\mathbb{1}_A \otimes C)]$ is a traceless operator, we have

$$\max_Q \text{Tr}\{\text{Tr}_B[(\varrho - \frac{\mathbb{1}_A}{2} \otimes \varrho_B)(\mathbb{1}_A \otimes C)]Q\} = \frac{1}{\sqrt{2}} \left\| \text{Tr}_B[(\varrho - \frac{\mathbb{1}_A}{2} \otimes \varrho_B)(\mathbb{1}_A \otimes C)] \right\|. \quad (\text{X8})$$

This identifies (X7) with the previous definition of the principal radius for two-qubit states (E1).

2. Remarks on other properties

Many properties of the critical radius can be obtained easily by adapting the proofs for 2-POVMs and the two-qubit system. This includes the scaling and the symmetry of the critical radius. As examples, we repeat these two statements and proofs.

a. *Scaling of the critical radius*

Theorem 35 (Scaling of the critical radius). *For any state ϱ and any $\lambda \geq 0$, we have*

$$R_n^{-1}[\varrho] = \frac{1}{\lambda} R_n^{-1}[\lambda\varrho + (1-\lambda)\frac{\mathbb{1}_A}{d_A} \otimes \varrho_B]. \quad (\text{X9})$$

Proof. The proof is very simple. We first note that the numerator in the definition of $r_n^{-1}[\varrho, \mu]$ can be rewritten as $\sum_{i=1}^n \text{Tr}[\varrho E_i \otimes Z_i] - \frac{1}{d_A} \sum_{i=1}^n \text{Tr}[E_i] = \sum_{i=1}^n \text{Tr}[(\varrho - \frac{\mathbb{1}_A}{d_A} \otimes \varrho_B) E_i \otimes Z_i]$. Then upon transforming $\varrho \rightarrow \lambda\varrho + (1-\lambda)\frac{\mathbb{1}_A}{d_A} \otimes \varrho_B$, this numerator gets a factor of λ while the denominator is invariant. \square

b. *Continuous symmetry of the critical radius*

The Bloch hyperplane \mathcal{P} is the linear manifold of hermitian trace-1 operators acting on $\mathbb{C}^{d_A} \otimes \mathbb{C}^{d_B}$. For $U \in \text{U}(d_A)$, $V \in \text{GL}(d_B)$, consider the affine transformation from the Bloch hyperplane of the joint system into itself $\varphi_{(U,V)} : \mathcal{P} \rightarrow \mathcal{P}$, defined by

$$\varphi_{(U,V)}(X) = \frac{(U \otimes V)X(U^\dagger \otimes V^\dagger)}{\text{Tr}[(U \otimes V)X(U^\dagger \otimes V^\dagger)]}. \quad (\text{X10})$$

for $X \in \mathcal{P}$. This is a group action of $\text{U}(d_A) \times \text{GL}(d_B)$ on \mathcal{P} . Note that $\varphi_{(U,V)}$ conserves the positivity, thus also maps the set of (bipartite) proper states into itself.

Theorem 36 (Continuous symmetry of the critical radius). *For any state ϱ and $U \in \text{U}(d_A)$, $V \in \text{GL}(d_B)$, we have $R_n[\varrho] = R_n[\varphi_{(U,V)}\varrho]$.*

The proof of this theorem then goes very similarly to the proof of Theorem 10, provided the following lemma is used instead of Lemma 9.

Lemma 37. *Consider a given state ϱ , a given probability measure (LHS ensemble) μ satisfying the minimal requirement $\int d\mu(\sigma)\sigma = \varrho_B$. For $U \in \text{U}(d_A)$ and $V \in \text{GL}(d_B)$, we denote $\tilde{\varrho} = \varphi_{(U,V)}(\varrho)$. Note that there exists a unique probability measure $\tilde{\mu}$ on \mathcal{B}_B defined by*

$$\int d\tilde{\mu}(\sigma)f(\sigma) = \frac{1}{\text{Tr}(V\varrho_B V^\dagger)} \int \frac{d\mu \circ \varphi_{V^{-1}}(\sigma)}{\text{Tr}[V^{-1}\sigma(V^{-1})^\dagger]} f(\sigma) \quad (\text{X11})$$

for all continuous functions f . Then $\tilde{\mu}$ satisfies the minimal requirement for $\tilde{\varrho}$ and $r_n[\varrho, \mu] = r_n[\tilde{\varrho}, \tilde{\mu}]$.

Proof. (i) The proof that $\tilde{\mu}$ satisfies the minimal requirement for $\tilde{\varrho}$ goes exactly as the proof of Lemma 9.

(ii) Now we prove that $r_n[\varrho, \mu] = r_n[\tilde{\varrho}, \tilde{\mu}]$. Using the definition (X3), we have $r_n^{-1}[\tilde{\varrho}, \tilde{\mu}]$ as

$$\sup_{Z,E} \frac{\sum_{i=1}^n \text{Tr}[\tilde{\varrho}(E_i \otimes Z_i)] - \frac{1}{d_A} \sum_{i=1}^n \text{Tr}(E_i) \text{Tr}(\tilde{\varrho}_B Z_i)}{\int d\tilde{\mu}(\sigma) \max_i \langle \tilde{Z}_i, P \rangle - \frac{1}{d_A} \sum_{i=1}^n \text{Tr}(E_i) \text{Tr}(\tilde{\varrho}_B Z_i)}. \quad (\text{X12})$$

Now using the definition of $\tilde{\mu}$, we find $\int d\tilde{\mu}(\sigma) \max_i \langle \tilde{Z}_i, \sigma \rangle$ to be

$$\frac{1}{\text{Tr}(V\varrho_B V^\dagger)} \int \frac{d\mu \circ \varphi_{V^{-1}}(\sigma)}{\text{Tr}(V^{-1}\sigma(V^{-1})^\dagger)} \max_i \langle \tilde{Z}_i, \sigma \rangle. \quad (\text{X13})$$

Upon making the transformation of variable $\sigma = \varphi_V(\tau)$, this becomes

$$\frac{1}{\text{Tr}(V\varrho_B V^\dagger)} \int d\mu(\tau) \max_i \text{Tr}(V^\dagger Z_i V \tau). \quad (\text{X14})$$

The denominator of the expression under the supremum in (X12) can then be written as

$$\int d\mu(\sigma) \max_i \langle \tilde{Z}_i, \sigma \rangle - \frac{1}{d_A} \sum_{i=1}^{d_A} \text{Tr}(E_i) \text{Tr}(\varrho_B \tilde{Z}_i), \quad (\text{X15})$$

where $\tilde{Z}_i = V^\dagger Z_i V$. Now using the definition of $\tilde{\varrho}$, the numerator can be written as

$$\sum_{i=1}^n \text{Tr}[\varrho(\tilde{E}_i \otimes \tilde{Z}_i)] - \frac{1}{d_A} \sum_{i=1}^{d_A} \text{Tr}(\tilde{E}_i) \text{Tr}(\varrho_B \tilde{Z}_i). \quad (\text{X16})$$

where $\tilde{E}_i = U^\dagger E_i U$. So the principal radius (X12) can be written as

$$\sup_{\tilde{Z}, \tilde{E}} \frac{\sum_{i=1}^n \text{Tr}[\varrho(\tilde{E}_i \otimes \tilde{Z}_i)] - \frac{1}{d_A} \sum_{i=1}^{d_A} \text{Tr}(\tilde{E}_i) \text{Tr}(\varrho_B \tilde{Z}_i)}{\int d\mu(\sigma) \max_i \langle \tilde{Z}_i, \sigma \rangle - \frac{1}{d_A} \sum_{i=1}^{d_A} \text{Tr}(\tilde{E}_i) \text{Tr}(\varrho_B \tilde{Z}_i)}, \quad (\text{X17})$$

where we have used $\text{Tr}(E_i) = \text{Tr}(\tilde{E}_i)$. Since the set of (\tilde{Z}, \tilde{E}) are the same as that of (Z, E) , this expression in fact coincides with the definition of $r_n^{-1}[\varrho, \mu]$. \square

Appendix Y: On the relation between PVMs and POVMs

Armed with the newly defined concepts, we now discuss the question of the equivalence of different classes of measurements in quantum steering, in particular of PVMs and POVMs. Because POVMs of n outcomes constitute a subset of POVMs of $n+1$ outcomes, we have a decreasing chain $r_2[\varrho, \mu] \geq r_3[\varrho, \mu] \geq \dots$. As a consequence, the critical radii also form a decreasing chain $R_2[\varrho] \geq R_3[\varrho] \geq \dots$. Since the extreme POVMs have at most d_A^2 non-empty outcomes, both of these two chains turn into equalities at $n = d_A^2$. We denote $R_{\text{POVM}}[\varrho] = R_{d_A^2}[\varrho]$. Where does the critical radius for PVMs, here denoted $R_{\text{PVM}}[\varrho]$, fit into this chain? There has been a suspicion that $R_{d_A^2}[\varrho] = R_{\text{PVM}}[\varrho]$, or POVMs and PVMs are equivalent in quantum steering. Until now, there has been no concrete evidence whether this conjecture is true except for certain special states [27, 43].

Here restricted to two-qubit states, we investigate a stronger hypothesis: $r_{\text{POVM}}[\varrho, \mu] = r_{\text{PVM}}[\varrho, \mu]$ for all μ , which certainly implies that $R_{\text{POVM}}[\varrho] = R_{\text{PVM}}[\varrho]$. For

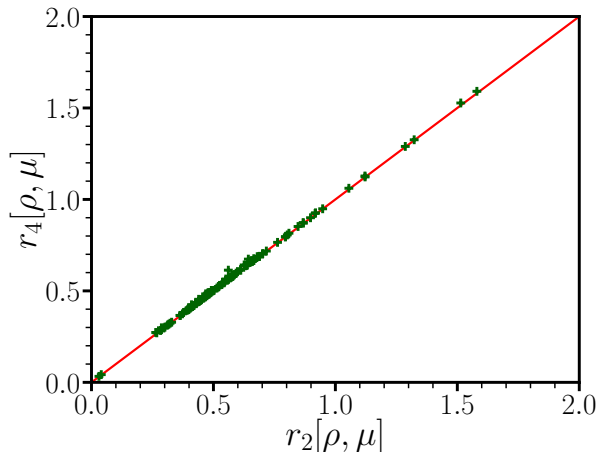


FIG. 9. The principal radii of random states and random LHS ensembles. While the values of $r_2[\varrho, \mu]$ are computed exactly, $r_4[\varrho, \mu]$ is estimated by a simulated annealing algorithm. If POVMs and PVMs were inequivalent, one would expect $r_4[\varrho, \mu]$ to be strictly smaller $r_2[\varrho, \mu]$ for certain ϱ and μ . Surprisingly, upto the numerical accuracy, we find that the estimated $r_4[\varrho, \mu]$ is equal to $r_2[\varrho, \mu]$, which implies that POVMs and PVMs are equivalent in a strong sense.

steering in two-qubit systems, since PVMs are equivalent to 2-POVMs (see, e.g., Ref. [20]), the above hypothesis amounts to ask if $r_2[\varrho, \mu] = r_4[\varrho, \mu]$. We test this hypothesis by sampling random states, constructing random LHS ensembles for each state. We then compute $r_2[\varrho, \mu]$ exactly. The computation of $r_4[\varrho, \mu]$ is performed by the simulated annealing algorithm (see below). Although the algorithm in principle only provides an upper bound of $r_4[\varrho, \mu]$, repeated runs indicate that it is close to the exact value of $r_4[\varrho, \mu]$. To our surprise, we find that in any single case, the obtained upper bound of $r_4[\varrho, \mu]$ approaches $r_2[\varrho, \mu]$ from above; see Figure 9. This strongly supports the hypothesis that $r_4[\varrho, \mu] = r_2[\varrho, \mu]$ at least for generic states ρ and generic LHS ensembles μ . This in turn supports the conjecture that for two-qubit systems, POVMs are equivalent to PVMs.

Remark 6. Let us make some remarks on the computation of the principal radius. From the previous section, it is clear that in actual computation, we are principally interested in the case $n = d_A^2$. While it is not obvious from the first look, the optimisation in the computation of $r_n[\varrho, \mu]$ can be limited to some simple subset of POVMs, namely rank-1 POVMs. We first note that $r_n^{-1}[\varrho, \mu]$ can be written as

$$\inf \{y : y \geq 0, y \geq F^{-1}[\varrho, \mu, Z, E]\}. \quad (\text{Y1})$$

Then since the denominator of $F^{-1}[\varrho, \mu, Z, E]$ is positive,

we can write $r_n[\varrho, \mu]$ as

$$\sup \{x : x \geq 0, \int d\mu(\sigma) \max_i \langle Z_i, \sigma \rangle \geq \sum_{i=1}^n \text{Tr}[\varrho_x E_i \otimes Z_i]\}, \quad (\text{Y2})$$

where $\varrho_x = x\varrho + (1-x)(\mathbb{1}_A/d_A) \otimes \varrho_B$. The second inequality is required to hold for all POVMs E and arbitrary composite operators Z . Note that this inequality is precisely the condition for ϱ_x to be unsteerable with LHS ensemble μ , c. f. equation (X1). Then we know that it holds for all POVMs E if it holds for all rank-1 POVMs; see, e.g., Ref. [44].

Now the optimisation (X3) to compute $r_n[\varrho, \mu]$ when limiting E to rank-1 POVMs is completely similar to the computation of the gap function in Ref. [27]. We refer to Ref. [27] for the detailed description of the simulated annealing algorithm.